Prescribed-Time Safety Design for Strict-Feedback Nonlinear Systems

Imoleayo Abel, Drew Steeves, Miroslav Krstić, *Fellow, IEEE*, and Mrdjan Janković, *Fellow, IEEE*

***Abstract*—Safety in dynamical systems is commonly pursued using control barrier functions (CBFs) which enforce safety-constraints over the entire duration of a system's evolution. We propose a prescribed-time safety (PTSf) design which enforces safety only for a finite time of interest to the user. While traditional CBF designs would keep the system away from the safe set longer than necessary, our PTSf design lets the system reach the boundary of the safe set by the prescribed time and obey the operator's intent thereafter. To emphasize the capability of our design for safety constraints with high relative degrees, we focus our exposition on strict-feedback systems where the safety condition is defined for the state furthest from the control input. In contrast to existing CBF-based methods for high relative degree constraints, our approach involves choosing explicitly specified gains (instead of class $\mathcal{K}$ functions), and, with the aid of backstepping, operates in the entirety of the original safe set with no additional restriction on the initial conditions. With QP being employed in the design, in addition to backstepping and CBFs with a PTSf property, we refer to our design as a QP-backstepping PT-CBF design. We include some numerical examples to illustrate the performance of our design.**

***Index Terms*—Automotive control, control theory, nonlinear control systems.**

I. Introduction

A. High Relative Degree CBFs

CONTROL barrier functions (CBFs) have become a popular tool for synthesizing safe controllers for dynamical systems and have been used in a wide range of problem domains, such as multiagent robotics [1], [2], [3], robust safety [4], [5], [6], automotive systems [7], [8], [9], delay systems [10], [11], [12], [13], and stochastic systems [14], [15], [16] to mention a few. First defined in [17] and later refined and popularized by the seminal papers [8], [18], CBFs are often employed in a "safety filter" framework where they are used for generating safe control overrides for a potentially unsafe nominal controller. In essence, a nominal controller is designed to achieve a desired performance objective, and a CBF-based control override is used whenever the nominal controller is at risk of making the system unsafe.

In its initial conception [8], [17], CBFs were specified for safety constraints of relative degree one, i.e., constraints whose time derivative depend explicitly on the input. The extension of CBFs to constraints with high relative degree (hi-rel-deg CBFs) was first studied independently in [19] and [20] with much progress following in [21], [22], [23], and [24]. In [20], the extension was limited to the relative degree two case, and in [19], where CBFs of arbitrarily hi-rel-deg was introduced; its usage for a relative degree r case involves choosing $r-1$ bounded, positive definite functions that satisfy additional derivative conditions [19, eq. (26)]: a requirement that limits the utility of [19] for significantly hi-rel-deg constraints. A similar limitation applies to more recent treatment [23] which requires choosing and tuning r class-$\mathcal{K}$ functions, whose choice determines the subset of the original safe set that is kept forward invariant. Building off [20], exponential CBFs were reported in [21] and allowed the use of simple linear control tools to design CBFs for hi-rel-deg constraints.

B. Nonovershooting Control Roots of High Relative Degree CBFs

Preceding the development of CBFs in [8], [17], and [21], a design for stabilization to an equilibrium point *at* the barrier was introduced, under the name "nonovershooting control," in the 2006 paper [25]. This design possesses all the attributes of a safety design with a CBF of a *uniform* and hi-rel-deg[1] with only the QP step absent since, for stabilization at the barrier, QP is subsumed in the stabilization design (the nominal feedback and the safety filtered feedback are the same).

The interest in nonovershooting control in the 1990s came from applications—spacecraft docking, aerial refueling, machining, etc.—with no margin for error in downward setpoint regulation. The nonovershooting control problem for linear systems, albeit mostly for zero initial conditions and nonzero setpoints, was solved in [26], [27], and [28].

Krstic and Bement [25] introduced the following two ideas (translated to the current CBF terminology). First, for a system with a hi-rel-deg CBF, a backstepping transformation into a particular target system in the form of a chain of first-order CBF subsystems (resulting in all real poles in the linear case) is performed. Second, in order to ensure that all the CBF "states"

Manuscript received 12 April 2023; revised 7 August 2023; accepted 15 October 2023. Date of publication 20 October 2023; date of current version 29 February 2024. This work was supported in part by NSF under Grant ECCS-2151525 and in part by ONR under Grant N00014-23-1-2376. Recommended by Associate Editor Aneel Tanwani. *(Corresponding author: Drew Steeves.)*

Imoleayo Abel, Drew Steeves, and Miroslav Krstić are with the Department of Mechanical and Aerospace Engineering, University of California, San Diego, CA 92093-0411 USA (e-mail: iabel@ucsd.edu; dsteeves@ucsd.edu; krstic@ucsd.edu).

Mrdjan Janković is with the Ford Research and Advanced Engineering, Birmingham, MI 48009 USA (e-mail: mrdjan_lt@earthlink.net).

Digital Object Identifier 10.1109/TAC.2023.3326393

[1]Uniformity of the CBF's relative degree gives the equivalence of a general control-affine system with the strict-feedback class and the convertibility of the safe set, given by the CBF positivity constraint, into a semiinfinite interval constraint for the first state of the strict-feedback system.

of this chain begin and remain positive, the positivity of their initial values is ensured by choosing the backstepping gains in accordance with the initial conditions so the entire CBF chain is initialized positively.

This chain structure and the gain selection of [[25], eqs. (12) and (13)], regarded through the lens of pole placement, were independently discovered in the 2016 paper [[21], Cor. 2]. Likewise, the nonlinear damping choices in the CBF chain in [[25], eqs. (53) and (54)] were independently proposed in the 2019 paper [23]. In addition, pursued in [25], but not in [21] and [23], was a form of input-to-state safety (ISSf) in the presence of disturbances. This notion, though not explored for hi-rel-deg CBFs, is rigorously conceived in [5].

Inspired by nonovershooting control under disturbances in [25], i.e., by stabilization to an equilibrium at the barrier along with ISSf, mean-square stabilization of stochastic nonlinear systems to an equilibrium at the barrier, along with a guarantee of nonviolation of the barrier in the mean sense, is solved in [29].

With a nearly negligible QP modification, the stabilizing feedbacks in [25] can be used in safety filters. Hence, backstepping generates a safety filter with explicit tuning variables that dictate the exponential approach to the barrier.

C. Prescribed-Time Safety (PTSf)

Recent advances in prescribed-time stabilization (PTS) [30] have resulted in time-varying backstepping controllers that guarantee settling times independent of initial conditions. Extensions have been developed to stochastic nonlinear systems [31], infinite-dimensional systems [32], [33], [34], and even coupled systems with finite/infinite-dimensional subsystems [35], [36], [37]. PTS is a subset of both the finite-time [38] and fixed-time [39] notions (i.e., stronger than both).

The success in achieving stabilization in prescribed time, independent of initial conditions, inevitably raises the question of pursuing the safety counterpart of the same notion. Yet, the two notions differ notably: while PTS guarantees that the state *reaches the equilibrium no later* than a prescribed time T, PTSf guarantees that the state *cannot reach the boundary of the safe set sooner* than a prescribed time T. The utility of PTSf stems from it enforcing a less conservative notion of safety than exponential safety (ESf) does. PTSf removes the infinite-time safety restrictions that ESf requires, allowing the system to operate at or beyond the barrier's proximity after time T. In automotive research, many dangers and rules are finite-time in nature, such as static obstacles that are eventually passed by the vehicle, and traffic lights that periodically turn green. For robot–human handover applications [40], the handover time is finite, and employing ESf means that the handover in never fully completed: it is only completed in an approximate sense. PTSf can enforce safety until the moment that the object is passed from robot to human.

We distinguish our notion of PTSf from recently defined notions of fixed- and finite-time safety (FxTSf/FnTSf) in [41]. In PTSf, safety is enforced only for a fixed time duration T, after which the system is allowed to enter the unsafe set, as dictated by the nominal system behavior. In contrast, FxTSf enforces safety *indefinitely* and acts in a manner where, whenever the safety filter kicks in and the nominal system behavior is overridden for a duration of T time units, the system is necessarily brought to the boundary of the safe-set at the end of that time duration. FnTSf acts similarly as FxTSf, but the time duration T is dependent on the state and nominal control input at the time the safety override kicks in. Furthermore, PTSf is also different from the notions of limited duration safety [42] and periodic safety using fixed-time CBFs [43]. Specifically, Garg et al. [43] introduced the notion of periodic safety, where the objective is to keep a system safe for *all times* while enforcing that it periodically (with time period T) visits a goal set *inside* the safe set. In [42], the notion of limited duration safety was studied, and like PTSf it implies that a system is kept safe only for a limited duration T. While [42] restricts the set of initial conditions—a set that shrinks as T increases [42, Rk. 2]—to be a strict subset of the safe set [42, eq. (3)], our notion of PTSf places no restriction on the initial conditions of the system. Recently, Kong et al. [44] introduced an adaptive tracking design for systems with output constraints occurring in a limited time interval. Unique to the design in [44] is the accommodation of limited-duration safety constraints that do not necessarily begin at the initial time of system evolution. However, the results in [44] are stated for constraints that are linear in the system output (PTSf permits nonlinear safety constraints). Furthermore, the reference trajectory being tracked is assumed to reside completely inside of the safe set, which is not the case for PTSf, where the nominal objective is allowed to be unsafe during the duration where safety is desired.

Finally, two distinct features of the time-varying backstepping technique make it attractive for use in safety filter design. The first is that, compared to ESf designs, the PTSf filters designed with time-varying backstepping do not exhibit large transients when the safety filter overrides the nominal controller. This is not the case for ESf filters with rapid decay rates: the so-called "peaking" phenomenon [45], [46], [47] is exhibited, which can cause some of the states to become very large near the initialization time (see Section V-A1), before rapidly converging to the equilibrium. This behavior can cause large state-derivatives, which, e.g., is undesirable in vehicle systems where maneuvers causing large acceleration and its derivative, jerk, can be dangerous. Moreover, when employing a state feedback controller, there is a direct consequence on the actuator when allowing large transients. PTSf safety filter designs avoid peaking by using small gains near initialization time that only grow large as the state decays. In essence, PTSf behaves like a smooth, automatic transition from slow ESf at the initialization time to fast ESf as time approaches the terminal time. The second feature making time-varying backstepping attractive is the behavior of the convergence it achieves near the terminal time. PTSf achieves convergence with "infinitely-soft" landing, that is, the state and *all* of its derivatives converge to the equilibrium by the terminal time. This feature occurring in finite time is unique to PTSf, and is desirable because it can ensure, e.g., safety maneuvers with zero jerk by the terminal time. In contrast, nonsmooth convergence (for example, a vehicle's position—but neither its velocity nor acceleration—converging continuously to a setpoint) at the terminal time has a direct consequence on its payload and passengers.

Among all classes of nonlinear systems, strict-feedback systems most commonly arise. Our PTSf design for vector strict-feedback systems is applicable to all fully actuated robotic and vehicular systems employing electric motors, hydraulic actuators, or propulsion devices. As we are pursuing a general systematic design for handling safety constraints for high-rel.-degree systems, we focus on strict-feedback systems; further

investigation is required to handle underactuated systems and other system structures.

D. Contributions

1) Time-varying backstepping design of *explicit* controllers that enforce state constraints of hi-rel-deg only for a *fixed* time duration. This is in contrast to [42], where limited-duration safe policies are *learned* via value function learning, and [41] where state-constraints are enforced *indefinitely*. Practically speaking, explicit state-feedback controllers are transparent in design and computationally inexpensive, and limited-duration safe policies are often encountered in controls applications.
2) By virtue of our particular time-varying design, the state-constrained controllers exhibit moderate transients, in contrast to time-invariant variations [21] that are tuned for similar system performance (see Section V-A1 for details). For mechanical systems where large transients mean causing acceleration and jerk in excess of allowable values, our time-varying approach is of practical importance.
3) Relative to the result in [41] on finite/fixed-time safety via homogeneous feedback for scalar chain-of-integrators with *linear* half-space state constraints, our PTSf design is simpler, and applicable to a more general class of vector strict-feedback systems with *nonlinear* state constraints, making it amenable to, for example, vehicular bicycle models with circle-to-circle barrier constraints, both of which are nonlinear.

E. Difference (Added Value) Relative to the Paper's Conference Version

This article is a journal version of our conference paper [48]. Per TAC policy,[2] the journal version's *added value* comprises a generalization from single-input, scalar chain-of-integrator systems with linear constraints to multiinput, vector strict-feedback systems with nonlinear constraints; updated and more detailed analysis and proofs; the inclusion of omitted proofs for Lemmas 2 and 3; theoretical discussions of solution existence after the terminal time and PTSf for initially unsafe systems; and lastly, two additional numerical examples. All of these additions and updates constitute an additional eight pages relative to the conference version.

F. Organization

The rest of this article is organized as follows. Section II contains the problem description alongside some brief preliminaries. In Section III, we present our QP-backstepping PT-CBF control design methodology. Our main result and its proof are included in Section IV, where we also discuss PTSf for initially unsafe systems. Section V includes three numerical examples with which we compare our design to existing constant-gain ESf designs. Finally, Section VI concludes this article.

[2][Online]. Available: http://ieeecss.org/publication/transactions-automatic-control/author-info, Section III, third paragraph

II. Problem Description and Preliminaries

We study vector strict-feedback systems of the following form:

$$\begin{aligned}\dot{\mathbf{x}}_i(t) &= \mathbf{x}_{i+1}(t) + \varphi_i(\underline{\mathbf{x}}_i(t)), \quad i = 1, \dots, n-1\\ \dot{\mathbf{x}}_n(t) &= B(\underline{\mathbf{x}}_n(t))u(t) + \varphi_n(\underline{\mathbf{x}}_n(t))\\ y(t) &= h(\mathbf{x}_1(t)), \qquad\qquad t \geq t_0\end{aligned} \tag{1}$$

where $t_0 \geq 0$ is the initialization time, $\mathbf{x}_i \in \mathbb{R}^m$ are vector-valued states, and $\underline{\mathbf{x}}_i$ represents the column vector

$$\underline{\mathbf{x}}_i = \begin{bmatrix}\mathbf{x}_1\\ \vdots\\ \mathbf{x}_i\end{bmatrix} \in \mathbb{R}^{mi} \tag{2}$$

with $\underline{\mathbf{x}}_n$ and $\mathbf{x}$ used interchangeably. The function $u \in \mathbb{R}^m$ is the Lebesgue-integrable input, and the functions $\varphi_i : \mathbb{R}^{mi} \to \mathbb{R}^m$ and $B : \mathbb{R}^{mn} \to \mathbb{R}^{m\times m}$ are defined as

$$\varphi_i(\underline{\mathbf{x}}_i) := \begin{bmatrix}\varphi_{i,1}(\underline{\mathbf{x}}_i)\\ \vdots\\ \varphi_{i,m}(\underline{\mathbf{x}}_i)\end{bmatrix} \tag{3}$$

$$B(\underline{\mathbf{x}}_n) = \begin{bmatrix}\beta_{1,1}(\underline{\mathbf{x}}_n) & \dots & \beta_{1,m}(\underline{\mathbf{x}}_n)\\ \vdots & & \vdots\\ \beta_{m,1}(\underline{\mathbf{x}}_n) & \dots & \beta_{m,m}(\underline{\mathbf{x}}_n)\end{bmatrix}. \tag{4}$$

Assumption 1: The matrix $B(\underline{\mathbf{x}}_n)$ is nonsingular for all $\underline{\mathbf{x}}_n \in \mathbb{R}^{mn}$. In addition, for each $i = 1, \dots, n$, the functions $\varphi_{i,j}(\underline{\mathbf{x}}_i) : \mathbb{R}^{mi} \to \mathbb{R},\ j = 1, \dots, m$ are $n - i$ times differentiable.

The safety objective is to keep the scalar output $y(t)$ positive for an a priori prescribed time $T > 0$ provided that $y(t_0)$ is positive; that is, we want

$$y(t_0) > 0 \Rightarrow y(t) > 0 \quad \forall t \in [t_0, t_0 + T)\,. \tag{5}$$

This can be interpreted as enforcing system safety (characterized by the positivity of $y(t)$) over the *finite* time horizon $[t_0, t_0 + T)$, where T is a terminal time that can be a priori prescribed. Geometrically, the closure of the inequality (5) describes the closed safe set $\mathcal{S} := \{\mathbf{x} : y(t) \geq 0\}$, where the system can safely operate during the time horizon $[t_0, t_0 + T]$. The meaning of the terminal time varies between applications: for example, it can represent the robot–human handover time, the time at which a traffic light signals green, or the time at which an autonomous vehicle passes an occlusion in the road. As is the case in many safety-critical systems, the control input will be filtered through a so-called safety filter which overrides a nominal control input u_{nom} whenever it violates conditions that prevent $y(t)$ from becoming negative before time $t_0 + T$. We note here that under certain additional assumptions to be discussed later, the control design methodology we shall present also achieves the dual task of bringing the system to safety in no later than T time units in the case that the system starts unsafe. That is, it achieves

$$y(t_0 + T) \geq 0 \quad \text{if } y(t_0) \leq 0. \tag{6}$$

Lastly, we state our assumption on the output map $h : \mathbb{R}^m \to \mathbb{R}$ in (1).

Assumption 2: The function $h : \mathbb{R}^m \to \mathbb{R}$ is n times differentiable and satisfies

$$\frac{\partial h}{\partial \mathbf{x}_1} \neq 0 \quad \forall\, \mathbf{x}_1 \in \{\chi \in \mathbb{R}^m \mid h(\chi) \geq 0\}\,. \tag{7}$$

A. Coordinate Transformation

The first step in our design is to transform the system (1) into a vector chain of integrators using the following state transformation:

$$\boldsymbol{\alpha}_0 = 0 \tag{8}$$

$$\boldsymbol{\alpha}_i(\underline{\mathbf{x}}_i) = -\varphi_i(\underline{\mathbf{x}}_i) + \sum_{j=1}^{i-1} \frac{\partial \boldsymbol{\alpha}_{i-1}}{\partial \mathbf{x}_j}\left(\mathbf{x}_{j+1} + \varphi_j(\underline{\mathbf{x}}_j)\right) \tag{9}$$

$$i = 1, \ldots, n$$

$$\mathbf{z}_i = \mathbf{x}_i - \boldsymbol{\alpha}_{i-1}, \qquad i = 1, \ldots, n \tag{10}$$

with input

$$u = B^{-1}(\underline{\mathbf{x}}_n)\left(v + \boldsymbol{\alpha}_n\right) \tag{11}$$

which leads to

$$\begin{aligned} \dot{\mathbf{z}}_i(t) &= \mathbf{z}_{i+1}(t), \quad i = 1, \ldots, n-1 \\ \dot{\mathbf{z}}_n(t) &= v(t), \\ y(t) &= h(\mathbf{z}_1(t)), \quad t \geq t_0. \end{aligned} \tag{12}$$

We note that the original output in (1) and the transformed output in (12) are equivalent since $\mathbf{z}_1 = \mathbf{x}_1$, and therefore, we shall focus our PTSf design on the system (12) by designing the input v that enforces positivity of $y(t)$, and use (11) to recover the input u for the original strict-feedback system. In addition, since our PTSf designs will be for the transformed system (12), we will transform any Lebesgue-integrable nominal control function u_{nom} applied to the original system (1) by using

$$v_{\text{nom}} = B(\underline{\mathbf{x}})u_{\text{nom}} - \boldsymbol{\alpha}_n. \tag{13}$$

Our safety filter will be applied to this transformed nominal input.

B. Preliminaries

Our PTSf designs will be generated by the following "blow-up" function:

$$\mu_m(t - t_0, T) = \frac{1}{\nu^m(t - t_0, T)}, \quad t \in [t_0, t_0 + T) \tag{14}$$

for $m \in \mathbb{N}_{\geq 2}$ and the *terminal time* $T > 0$, where

$$\nu(t - t_0, T) := \frac{T + t_0 - t}{T} \tag{15}$$

decays linearly from one to zero by the terminal time. We denote by $m^{\overline{k}}$ the *rising factorial* for $m, k \in \mathbb{N}$, that is

$$m^{\overline{k}} := m(m+1)\cdots(m+k-1) \tag{16}$$

the derivatives of μ_m are

$$\mu_m^{(i)}(t - t_0, T) = \frac{m^{\overline{i}}}{T^i}\mu_{m+i}(t - t_0, T). \tag{17}$$

For the rest of this article, we shall use μ_m and $\mu_m(t)$ to denote $\mu_m(t - t_0, T)$ for brevity when there is no confusion.

We denote by $\mathcal{P}^n(x)$ an nth-order polynomial in x.

III. QP-Backstepping PT-CBF Design for Nth-Order Vector Chain-of-Integrators

We recall the system of interest

$$\begin{aligned} \dot{\mathbf{z}}_i(t) &= \mathbf{z}_{i+1}(t), \quad i = 1, \ldots, n-1 \\ \dot{\mathbf{z}}_n(t) &= v(t) \\ y(t) &= h(\mathbf{z}_1(t)), \quad t \geq t_0. \end{aligned} \tag{18}$$

We aim to design a safety filter such that $y(t) > 0$ uniformly over the finite time horizon $[t_0, t_0 + T)$; that is, we wish to only enforce safety while it may be needed. Our design proceeds with a time-varying backstepping transformation defined as follows, where we suppress the time-dependency of μ_2

$$h_1(\mathbf{z}_1) = h(\mathbf{z}_1) \tag{19}$$

$$h_i(\underline{\mathbf{z}}_i, t) = \sum_{j=1}^{i-1} \frac{\partial h_{i-1}}{\partial \mathbf{z}_j}\mathbf{z}_{j+1} + \frac{\partial h_{i-1}}{\partial t} + c_{i-1}\mu_2 h_{i-1}$$

$$i = 2, \ldots, n \tag{20}$$

where c_i, $i = 1, \ldots, n-1$ are positive design parameters to be determined, and the transformed states h_i's are called barrier functions to connote the desire to keep their values positive provided that their initial values $h_i(t_0)$ are positive, as is typical with standard CBFs [18]. As defined, the barrier functions h_i in (20) satisfy

$$\frac{d}{dt}h_i = -c_i\mu_2 h_i + h_{i+1}, \quad i = 1, \ldots, n-1 \tag{21}$$

and for the last barrier function h_n in the chain, we have

$$\frac{d}{dt}h_n(\underline{\mathbf{z}}_n, t) = \sum_{j=1}^{n-1} \frac{\partial h_n}{\partial \mathbf{z}_j}\mathbf{z}_{j+1} + \frac{\partial h_n}{\partial t} + \frac{\partial h_n}{\partial \mathbf{z}_n}v(t) \tag{22}$$

which includes the control input $v(t)$ in the last term. Therefore, we shall require that the input $v(t)$ preserves the positivity of h_n if $h_n(t_0) > 0$. In particular, we shall permit only inputs $v(t)$ that ensure that the total time derivative $\frac{d}{dt}h_n$ satisfies the time-varying *barrier constraint*

$$\frac{d}{dt}h_n + c_n\mu_2 h_n \geq 0 \tag{23}$$

which we will later show is a sufficient condition for enforcing the positivity of h_n (and consequently $h_{n-1}, \ldots, h_1$) over a time interval of length T, provided that $h_i(t_0) > 0$, $i = 1, \ldots, n$. To achieve (23), we override any nominal control input $v_{\text{nom}}(t)$ with the closest (in the Euclidean sense) input $v_{\text{safe}}(t)$ that ensures $\frac{d}{dt}h_n + c_n\mu_2 h_n \geq 0$ is satisfied. This is equivalent to solving the quadratic programming (QP) problem

$$\begin{aligned} v_{\text{safe}} = \arg\min\nolimits_{w \in \mathbb{R}^m} \; & ||w - v_{\text{nom}}||^2 \\ \text{s.t.} \quad & a + b^\top w \geq 0 \end{aligned} \tag{24}$$

where

$$a := c_n\mu_2 h_n + \sum_{j=1}^{n-1} \frac{\partial h_n}{\partial \mathbf{z}_j}\mathbf{z}_{j+1} + \frac{\partial h_n}{\partial t}$$

$$b^\top := \frac{\partial h_n}{\partial \mathbf{z}_n}. \tag{25}$$

Notice from (20) that the barrier functions h_i satisfy

$$\frac{\partial h_i}{\partial \mathbf{z}_i} = \frac{\partial h_{i-1}}{\partial \mathbf{z}_{i-1}} \tag{26}$$

$$\Rightarrow \frac{\partial h_i}{\partial \mathbf{z}_i} = \frac{\partial h_1}{\partial \mathbf{z}_1} \quad \forall i = 1, \ldots, n \tag{27}$$

and coupled with (25) and (7) in Assumption 2, we have

$$b^\top = \frac{\partial h_1}{\partial \mathbf{z}_1} \neq 0 \tag{28}$$

which guarantees that the QP problem (24) is always feasible. Applying the Karush–Kuhn–Tucker (KKT) optimality conditions to (24) then leads to the explicit solution

$$v_{\text{safe}} = \begin{cases} v_{\text{nom}}, & a + b^\top v_{\text{nom}} \geq 0 \\ v_{\text{nom}} - \frac{a + b^\top v_{\text{nom}}}{||b||^2} b, & \text{otherwise} \end{cases} \tag{29}$$

where we shall subsequently refer to the expression in the second branch as

$$v_{\text{override}} := v_{\text{nom}} - \frac{a + b^\top v_{\text{nom}}}{||b||^2} b. \tag{30}$$

The QP solution (29) can be written equivalently as

$$v_{\text{safe}} = v_{\text{nom}} + \frac{\max\{0, -a - b^\top v_{\text{nom}}\}}{||b||^2} b. \tag{31}$$

Altogether, the input applied to the system (18) to enforce safety only for a fixed-time interval T is

$$v(t) = \begin{cases} v_{\text{safe}}(t), & \text{if } t_0 \leq t < t_0 + T \\ g(t, v_{\text{nom}}(t), v_{\text{terminal}}, h_1(t_0 + T)) & \\ & \text{if } t \geq t_0 + T \end{cases} \tag{32}$$

where

$$v_{\text{terminal}} = \left(I - \frac{b(t_0 + T) b^\top (t_0 + T)}{||b(t_0 + T)||^2} \right) v_{\text{nom}}(t_0 + T) \tag{33}$$

for the "ramp" function

$$g(t, v_{\text{nom}}(t), v_{\text{terminal}}, h_1(t_0 + T))$$

$$:= \begin{cases} \Phi(t - t_0 - T, \bar{T}) v_{\text{terminal}} + (1 - \Phi(t - t_0 - T, \bar{T})) v_{\text{nom}}(t) & \\ \qquad \text{if } h_1(t_0 + T) = 0, \quad t_0 + T \leq t \leq t_0 + T + \bar{T} & \\ v_{\text{nom}}(t), \qquad \text{otherwise} & \end{cases} \tag{34}$$

where

$$\Phi(t - t_0 - T, \bar{T}) := e^{-(\mu_1 (t - t_0 - T, \bar{T}) - 1)} \tag{35}$$

and $\bar{T} > 0$ is a design parameter. The role of g in (32) is to ensure that the control law is continuous at $t = t_0 + T$ when control authority is transferred to the nominal control v_{nom}. A high-level illustration of the control flow for our design is shown in the block diagram in Fig. 1.

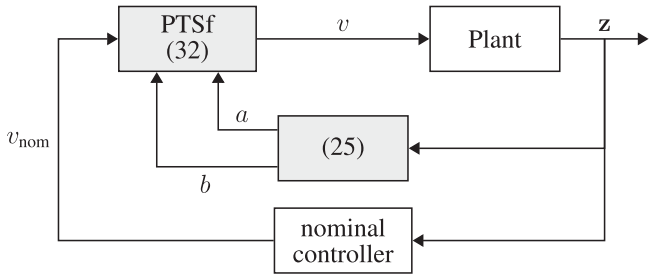

Fig. 1. Block diagram with PTSf filter generating input v which overrides a potentially unsafe nominal input v_{nom}.

With the safety filter (32), the barrier functions satisfy

$$\frac{d}{dt} h_i = -c_i \mu_2 h_i + h_{i+1}, \quad i = 1, \ldots, n-1 \tag{36}$$

$$\frac{d}{dt} h_n \geq -c_n \mu_2 h_n \tag{37}$$

for $t \in [t_0, t_0 + T)$. We can now state and prove our main result.

IV. Safety Theorem

Theorem 1: If the system (18) is initially safe and away from the barrier, that is, if $y(t_0) > \varepsilon > 0$, then the control law (32), (19)–(34) ensures that $y(t) > 0$ for all $t \in [t_0, t_0 + T)$ for the *initial* control gains

$$c_i > \max\{0, \underline{c}_i\}, \quad i = 1, \ldots, n-1$$

$$c_n > 0 \tag{38}$$

where

$$\underline{c}_i = -\frac{1}{h_i(\underline{\mathbf{z}}_i(t_0), t_0)} \left[\sum_{j=1}^{i} \frac{\partial h_i(\underline{\mathbf{z}}_i(t_0), t_0)}{\partial \mathbf{z}_j} \mathbf{z}_{j+1}(t_0) + \frac{\partial h_i(\underline{\mathbf{z}}_i(t_0), t_0)}{\partial t} \right]. \tag{39}$$

Moreover, the control law (32) is uniformly bounded provided that v_{nom} is continuous in t and Lipschitz in $\mathbf{z}$ (uniformly in t) [3] in the interval $[t_0, t_0 + T]$.

Remark 1: While not characterized in Theorem 1, if the safety filter overrides the nominal control input over the time interval $[t_0 + \bar{t}, t_0 + T)$ for some $\bar{t} < T$, then the convergence of the barrier functions to zero with be "infinitely soft": in other words, all of the derivatives $\frac{d^k}{dt^k} h_i(\underline{\mathbf{z}}_i, t)$, $k \in \mathbb{N}$, will also converge to zero by the terminal time $t_0 + T$. See Section IV-A, and in particular, (69) and (72) for the mathematical treatment of this "infinitely soft" convergence.

We now pursue a proof of Theorem 1.

A. Proof of Theorem 1

The structure of our proof comes in two parts: one to establish positivity of $y(t)$ for $t \in [t_0, t_0 + T)$; and another to establish uniform boundedness of the controller which filters the nominal control input to enforce safety. While these two parts are

[3] The conditions on v_{nom} are such that the nominal system is well posed.

intimately connected, each part requires different treatments. To ensure positivity of $h_1(\mathbf{z}_1)$ for $t \in [t_0, t_0+T)$, it is enough to invoke the control barrier *constraint* (37) and the choice of control gains (38). On the other hand, due to the possible switches in control input between v_{nom} and v_{override} in (29), one must take care to ensure uniform boundedness of the input v_{override}, whose gains increase with time due to the presence of μ_2 in (30) via the a term *even when* $v = v_{\text{nom}}$. To this end, we first present the following commutativity property of the "blow-up" function (14) which we will leverage to show controller boundedness. To simplify our presentation, we take $t_0 = 0$ henceforth.

Lemma 2: For $m \in \mathbb{N}_{\geq 1}$ and $0 \leq \bar{t} \leq t < T$, the "blow-up" function (14) satisfies

$$\mu_m(t,T) = \mu_m(\bar{t},T)\mu_m(t-\bar{t},T-\bar{t}). \tag{40}$$

Proof: It follows directly from the definition (14)

$$\begin{aligned}\mu_m(t,T) &:= \frac{1}{\left(1-\frac{t}{T}\right)^m} \\ &= \frac{1}{\left(1-\frac{\bar{t}}{T}\right)^m}\frac{1}{\left(\frac{T-t}{T-\bar{t}}\right)^m} \\ &= \mu_m(\bar{t},T)\mu_m(t-\bar{t},T-\bar{t}).\end{aligned} \tag{41}$$

■

To demonstrate controller uniform boundedness, we must leverage the fact that the feedback law invokes PTSf whose convergence dominates the rate of divergence of the time-varying control gains in (30). To accomplish this, we characterize the following property of the closed-loop system.

Lemma 3: For $c > 0$, the ith derivative of the function

$$\xi_{j,k}(t,T) := e^{-c_j^k T(\mu_1(t,T)-1)} \tag{42}$$

satisfies

$$\begin{aligned}&\lim_{t\to T^-} \frac{d^i \xi_{j,k}(t,T)}{dt^i} \\ &\quad = \lim_{t\to T^-} \mathcal{P}^{2i}\left(\mu_1(t,T)\right)\xi_{j,k}(t,T) = 0,\ i \in \mathbb{N}.\end{aligned} \tag{43}$$

Proof: We compute the first derivative according to (17)

$$\frac{d\xi_{j,k}(t,T)}{dt} = -2c_j^k \mu_2(t,T) e^{-c_j^k T(\mu_1(t,T)-1)}. \tag{44}$$

An application of l'Hôpital's rule to (44) twice verifies (43) for $i = 1$, since

$$\begin{aligned}\lim_{t\to T^-} \frac{d\xi_{j,k}(t,T)}{dt} &= -2c_j^k e^{c_j^k T} \lim_{t\to T^-} \mu_2(t,T) e^{-c_j^k T \mu_1(t,T)} \\ &= -2c_j^k e^{c_j^k T} \lim_{\tau\to+\infty} \frac{\tau^2}{e^{-c_j^k T\tau}} = 0.\end{aligned} \tag{45}$$

For successive derivatives, we rely on the general Leibniz rule to study the time-varying structure of the expression

$$\begin{aligned}\frac{d^i \xi_{j,k}(t,T)}{dt^i} &= -2c_j^k \frac{d^{i-1}}{dt^{i-1}}\left(\mu_2(t,T)e^{-c_j^k T(\mu_2(t,T)-1)}\right) \\ &= -2c_j^k \sum_{l=0}^{i-1}\binom{i-1}{l}\mu_2^{(l)}(t,T)\frac{d^{i-l-1}\xi_{j,k}(t,T)}{dt^{i-l-1}} \\ &= -2c_j^k \sum_{l=0}^{i-1}\frac{2^{\bar{l}}}{T^l}\binom{i-1}{l}\mu_{2+l}(t,T)\frac{d^{i-l-1}\xi_{j,k}(t,T)}{dt^{i-l-1}}.\end{aligned} \tag{46}$$

We assume by induction that (43) holds for the $(i-1)$th derivative such that

$$\frac{d^{i-1}\xi_{j,k}(t,T)}{dt^{i-1}} = \mathcal{P}^{2(i-1)}\left(\mu_1(t,T)\right)\xi_{j,k}(t,T). \tag{47}$$

It follows from applying l'Hôpital's rule to (46) with (47) $i+2$ times that (43) holds for all $i \in \mathbb{N}$. ■

We can now proceed with the proof of Theorem 1, where we select $t_0 = 0$ for clarity.

Proof: We first pursue positivity of $y(t)$ under (32), (38), and (39). The system beginning from safety implies that $h_1(t_0) > 0$. We proceed by induction: suppose $h_i(t_0) > 0$ for some $i = 1, \ldots, n-1$; it follows from (20) that

$$h_{i+1}(t_0) = c_i h_i(t_0) + \frac{dh_i}{dt}(t_0) \tag{48}$$

where we have used $\mu_2(t_0 - t_0, T) = 1$. Our *initial* control gains (38) and (39) are designed so that

$$c_i h_i(t_0) + \frac{dh_i}{dt}(t_0) > 0. \tag{49}$$

We now show that $h_i(t_0) > 0$ for all $i = 1, \ldots, n$ is a sufficient condition for nonnegativity of $h_i(t)$ for $t \in [t_0, t_0+T)$.

Applying the comparison lemma and variation of constants formula to (36) and (37) gives

$$\begin{aligned}h_i(t) &= h_i(t_0)e^{-c_i\int_{t_0}^t \mu_2(s)\,ds} + \int_{t_0}^t e^{-c_i\int_\tau^t \mu_2(s)\,ds} h_{i+1}(\tau)\,d\tau \\ &\quad i = 1, \ldots, n-1\end{aligned} \tag{50}$$

$$h_n(t) \geq h_n(t_0)e^{-c_n\int_{t_0}^t \mu_2(s)\,ds} > 0 \tag{51}$$

for $t \in [t_0, t_0+T)$. Substituting (51) into (50) for $i = n-1$ yields

$$\begin{aligned}h_{n-1}(t) &\geq h_{n-1}(t_0)e^{-c_{n-1}\int_{t_0}^t \mu_2(s)\,ds} \\ &\quad + h_n(t_0)\int_{t_0}^t \Big[e^{-c_{n-1}\int_\tau^t \mu_2(s)\,ds} \\ &\quad \times e^{-c_n\int_{t_0}^\tau \mu_2(s)\,ds}\Big]\,d\tau \\ &\geq h_{n-1}(t_0)e^{-c_{n-1}\int_{t_0}^t \mu_2(s)\,ds} > 0.\end{aligned} \tag{52}$$

By using (51) and (52) and by proceeding by backward strong induction, it follows that

$$h_1(t) \geq h_1(t_0)e^{-c_1\int_{t_0}^t \mu_2(s)\,ds} \tag{53}$$

which implies

$$h_1(t) > 0 \tag{54}$$

for all $t \in [t_0, t_0+T)$.

We now pursue T-uniform boundedness of the the control law (32). We partition the time horizon $[0, T)$ into intervals for which the system is either deemed safe or unsafe according to

the safety filter by defining

$$t_k := \begin{cases} \min\{t_{k-1} < t \le T : v_{\text{nom}}(t) = v_{\text{override}}(\mathbf{z}, t)\} \\ \qquad\qquad\qquad\qquad \text{if it exists} \\ T, \qquad\qquad\qquad\qquad \text{otherwise} \end{cases} \tag{55}$$

for $k \in \mathbb{N}$ with $t_0 = 0$, where

$$[0, T) = \bigcup_{\substack{k \in \mathbb{N} \cup \{0\} \\ t_{k+1} \le T}} [t_k, t_{k+1}). \tag{56}$$

We have constructed this partition such that the control law (32) remains continuous at t_k, precluding Zeno behavior of the closed-loop system. Since the system is initially safe, $t_1 \neq T$ represents the first time that safety is enforced by (32). For $t \in [t_{2k}, t_{2k+1})$, $k \in \mathbb{N} \cup \{0\}$ and $t_{2k+1} \le T$, we define barrier functions

$$h_1^{2k}(\mathbf{z}_1) := h(\mathbf{z}_1(t)) \tag{57}$$

$$h_i^{2k}(\underline{\mathbf{z}}_i, t) := c_i^{2k} \mu_2(t - t_{2k}, T - t_{2k}) h_{i-1}^{2k}(\underline{\mathbf{z}}_{i-1}, t) + \frac{d}{dt} h_{i-1}^{2k}(\underline{\mathbf{z}}_{i-1}, t), \qquad i = 2, \dots, n \tag{58}$$

with c_i^{2k} to be specified later. It follows from (32) and (29) that during these intervals, the barrier functions satisfy

$$\frac{d}{dt} h_i^{2k} = -c_i^{2k} \mu_2(t - t_{2k}, T - t_{2k}) h_i^{2k} + h_{i+1}^{2k} \tag{59}$$

$$\frac{d}{dt} h_n^{2k} > -c_n^{2k} \mu_2(t - t_{2k}, T - t_{2k}) h_n^{2k} \tag{60}$$

for $i = 1, \dots, n-1$. Similarly, for $t \in [t_{2k-1}, t_{2k})$, $k \in \mathbb{N}$, and $t_{2k} \le T$, we define the barrier functions

$$h_1^{2k-1}(\mathbf{z}_1) := h(\mathbf{z}_1(t)) \tag{61}$$

$$h_i^{2k-1}(\underline{\mathbf{z}}_i, t) := c_i^{2k-1} \mu_2(t - t_{2k-1}, T - t_{2k-1}) h_{i-1}^{2k-1}(\underline{\mathbf{z}}_{i-1}, t) + \frac{d}{dt} h_{i-1}^{2k-1}(\underline{\mathbf{z}}_{i-1}, t), \qquad i = 2, \dots, n. \tag{62}$$

As before, it follows from (32), (29), and (62) that during these intervals, the barrier functions satisfy

$$\frac{d}{dt} h_i^{2k-1} = -c_i^{2k-1} \mu_2(t - t_{2k-1}, T - t_{2k-1}) h_i^{2k-1} + h_{i+1}^{2k-1} \tag{63}$$

$$\frac{d}{dt} h_n^{2k-1} = -c_n^{2k-1} \mu_2(t - t_{2k-1}, T - t_{2k-1}) h_n^{2k-1} \tag{64}$$

for $i = 1, \dots, n-1$.

We select $c_i^0 = c_i$ according to (38) and (39), and we select

$$c_i^k = c_i^{k-1} \mu_2(t_k - t_{k-1}, T - t_{k-1}), \quad k \in \mathbb{N}. \tag{65}$$

It follows by definition that $h_1^{2k}(t_{2k-1}) = h_1^{2k-1}(t_{2k-1})$ for $k \in \mathbb{N}$. Furthermore, by applying the initial gain selection (65) to (61) and (62) and comparing them to (57) and (58) at $t = t_{2k-1}$, we deduce that $h_i^{2k}(t_{2k-1}) = h_i^{2k-1}(t_{2k-1})$ for $i = 2, \dots, n$. The same treatment leads to the equalities $h_i^{2k}(t_{2k}) = h_i^{2k-1}(t_{2k})$ for $i = 1, \dots, n$. Hence, the initial gain selection (65) for each time partition in (56) ensures that the system dynamics remain continuous at every time. In fact, it simply tracks the growth of the "blow-up" function μ_2 over the time intervals.

Furthermore, we can leverage Lemma 2 and the initial gain selection (65) to show that

$$\prod_{k \in \mathbb{N}} c_i^k \mu_2(t - t_k, T - t_k) = \mu_2(t, T). \tag{66}$$

In other words, the barrier function design over the partitioned set (56) is consistent with the design (20)–(39).

For $t \in [t_{2k}, t_{2k+1})$, $k \in \mathbb{N} \cup \{0\}$, and $t_{2k+1} \le T$, the system is safe and the nominal control $v_{\text{nom}}(t)$—which we assume to be uniformly bounded (continuous over a compact time interval)—is being applied. For $t \in [t_{2k-1}, t_{2k})$, $k \in \mathbb{N}$, and $t_{2k} \le T$, we must estimate the size of the time-varying input $v_{\text{override}}(t)$ to verify that it is bounded.

To this end, we first study the stability of (63) and (64). We can solve (64) explicitly to obtain

$$h_n^{2k-1}(\underline{\mathbf{z}}_n, t) = e^{-c_n^{2k-1}(T - t_{2k-1})(\mu_1(t - t_{2k-1}, T - t_{2k-1}) - 1)} \times h_n^{2k-1}(\underline{\mathbf{z}}_n(t_{2k-1}), t_{2k-1}). \tag{67}$$

Whereas for $i = 1, \dots, n-1$, we have the relationship

$$h_i^{2k-1}(\underline{\mathbf{z}}_i, t) = e^{-c_i^{2k-1}(T - t_{2k-1})(\mu_1(t - t_{2k-1}, T - t_{2k-1}) - 1)} \times h_i^{2k-1}(\underline{\mathbf{z}}_i(t_{2k-1}), t_{2k-1}) + \int_{t_{2k-1}}^{t} \left[e^{-c_i^{2k-1} \int_\tau^t \mu_2(z - t_{2k-1}, T - t_{2k-1}) dz} \times h_{i+1}^{2k-1}(\underline{\mathbf{z}}_{i+1}(\tau), \tau) d\tau \right]. \tag{68}$$

We first study the limiting behavior of these functions when $t_{2k} = T$. We apply Lemma 3 to (67) to establish that successive derivatives of (67) will converge to zero by the terminal time

$$\lim_{t \to T^-} \frac{d^r h_n^{2k-1}(\underline{\mathbf{z}}_n, t)}{dt^r} = \lim_{t \to T^-} \mathcal{P}^{2r}\left(\mu_1(t, T)\right) \xi_{n,2k-1}(t - t_{2k-1}, T - t_{2k-1}) = 0 \tag{69}$$

for $r \in \mathbb{N} \cup \{0\}$. For $i = 1, \dots, n-1$, we use (68) to compute

$$\frac{d}{dt} h_i^{2k-1}(\underline{\mathbf{z}}_i, t) = h_{i+1}^{2k-1}(\underline{\mathbf{z}}_{i+1}, t) + h_i^{2k-1}(\underline{\mathbf{z}}_i(t_{2k-1}), t_{2k-1}) \frac{d}{dt} \xi_{i,2k-1}(t - t_{2k-1}, T - t_{2k-1}). \tag{70}$$

Moreover, since our design (38) together with the analysis (52) and (53) ensure that $h_i(\underline{\mathbf{z}}_i(t_{2k-1}), t_{2k-1}) > 0$ for $i = 1, \dots, n$, it follows by proceeding backward from (67) with (68) that

$$h_i^{2k-1}(\underline{\mathbf{z}}_n, t) \le \xi_{i,2k-1}(t - t_{2k-1}, T - t_{2k-1}) \times h_i^{2k-1}(\underline{\mathbf{z}}_i(t_{2k-1}), t_{2k-1}) + \min_{c_i^{2k-1}, \dots, c_n^{2k-1}} \left\{ \xi_i^{2k-1}(t - t_{2k-1}, T - t_{2k-1}) \right\} \times \sum_{j=i+1}^{n} \frac{(T - t_{2k-1})^j}{j!} h_j^{2k-1}(\underline{\mathbf{z}}_j(t_{2k-1}), t_{2k-1}). \tag{71}$$

By applying Lemma 3 to the second right-hand side term within (70), and by backward strong induction on (69) and (70),

we get for $r \in \mathbb{N} \cup \{0\}$ that

$$\begin{aligned}&\lim_{t\to T^-} \frac{d^r h_i^{2k-1}(\underline{\mathbf{z}}_i, t)}{dt^r} \\ &= \lim_{t\to T^-} \mathcal{P}^{2r}\left(\mu_1(t,T)\right) \max_{i\le j\le n}\left\{\xi_{j,2k-1}(t-t_{2k-1}, T-t_{2k-1})\right\} \\ &= 0, \qquad i = 1,\dots,n-1 \end{aligned} \tag{72}$$

where $\max_j\{\xi_j\}$ is well defined for all $t \in [t_{2k-1}, T)$ since the ordering of $\{\xi_{i,2k-1}\}_i$ is retained over the entire time interval. Hence, all of the derivatives of h_i^{2k-1} converge to zero at the terminal time with the rates given in (69) and (72).

Moreover, it is clear from the T-uniformly dominating behavior of the negative exponential in (67) and (68) that

$$\left|h_i^{2k-1}(\underline{\mathbf{z}}_i, t)\right| < +\infty \quad \forall\, t \in [t_{2k-1}, t_{2k}),\ i = 1,\dots,n. \tag{73}$$

Their time derivatives are also T-uniformly bounded by the same arguments. Hence, we have shown that when the nominal control input is overridden by the safety filter to enforce safety during $t \in [t_{2k-1}, t_{2k}), k \in \mathbb{N}$ and $t_{2k} \le T$, the time-varying backstepping design ensures that the barrier functions are bounded, and when $t_{2k} = T$, they converge very smoothly to zero by the terminal time: indeed, all of their derivatives also converge to zero by the terminal time.

We can now pursue T-uniform boundedness of the overriding controller, v_{override} in (30). Since $\frac{|b^\top v_{\text{nom}} b|}{\|b\|^2} \le \|v_{\text{nom}}\|$ by Cauchy–Schwarz, v_{override} is bounded provided that v_{nom} and a in (25) are bounded. The boundedness of v_{nom} follows from the assumption that it is T-uniformly continuous. To establish boundedness of a, we first establish that the components of the target states $\mathbf{z}_i$, $i = 2,\dots,n$ parallel to the vector b are driven to zero by the terminal time.

Lemma 4: For

$$\mathbf{z}_{i,\|}(t) := \frac{\langle \mathbf{z}_i(t), b\rangle}{\|b\|^2} b \tag{74}$$

denoting the parallel component of the target system state with respect to the vector b, we have

$$\lim_{t\to T^-} \mathbf{z}_{i,\|}(t) = \lim_{t\to T^-} \mathcal{P}\left(\mu_1(t,T)\right)\xi_{k,2k-1}(t) = 0 \tag{75}$$

for $i = 2,\dots,n$ and for all $t \in [t_{2k-1}, T)$.

Proof: We proceed by induction. Note that for $i = 2$, differentiating (19) yields

$$\frac{d}{dt}h_1(\mathbf{z}_1) = b^\top \mathbf{z}_2 = b^\top \mathbf{z}_{2,\|} \tag{76}$$

and an application of (72) yields (75). We assume the following form for the ith derivative of h_1, for $i \in \mathbb{N}_{\ge 1}$ which we later validate inductively

$$\begin{aligned}&\frac{d^i}{dt^i}h_1(\mathbf{z}_1) \\ &= b^\top \mathbf{z}_{i+1,\|} + \sum_{j=0}^{i-2}\sum_{k=0}^{j} \mathbf{z}_{i-j,\|}^\top \frac{d^{2+k}h_1(\mathbf{z}_1)}{d\mathbf{z}_1^{2+k}}\mathcal{P}^k(\underline{\mathbf{z}}_{2+j-k})\end{aligned} \tag{77}$$

where for $l \ge 2$, $\underline{\mathbf{z}}_l = \mathbf{z}_2,\dots,\mathbf{z}_l$. Differentiating once more yields

$$\begin{aligned}\frac{d^{i+1}}{dt^{i+1}}h_1(\mathbf{z}_1) &= b^\top \mathbf{z}_{i+2,\|} + \mathbf{z}_{i+1,\|}^\top \frac{d^2 h_1(\mathbf{z}_1)}{d\mathbf{z}_1^2}\mathbf{z}_2 \\ &+ \sum_{j=0}^{i-2}\sum_{k=0}^{j} \mathbf{z}_{(i+1)-j,\|}^\top \frac{d^{2+k}h_1(\mathbf{z}_1)}{d\mathbf{z}_1^{2+k}}\mathcal{P}^k(\underline{\mathbf{z}}_{2+j-k}) \\ &+ \sum_{j=0}^{i-2}\sum_{k=0}^{j+1} \mathbf{z}_{i-j,\|}^\top \frac{d^{2+k}h_1(\mathbf{z}_1)}{d\mathbf{z}_1^{2+k}}\widetilde{\mathcal{P}}^k(\underline{\mathbf{z}}_{2+j-k+1})\end{aligned} \tag{78}$$

where $\widetilde{\mathcal{P}}_k$ accounts for changes in the polynomials terms/coefficients that arise from the differentiation. Reindexing the terminal sum and absorbing the second term within (78) yields

$$\begin{aligned}&\frac{d^{i+1}}{dt^{i+1}}h_1(\mathbf{z}_1) \\ &= b^\top \mathbf{z}_{i+2,\|} + \sum_{j=0}^{i-1}\sum_{k=0}^{j} \mathbf{z}_{(i+1)-j,\|}^\top \frac{d^{2+k}h_1(\mathbf{z}_1)}{d\mathbf{z}_1^{2+k}}\mathcal{P}^k(\underline{\mathbf{z}}_{2+j-k})\end{aligned} \tag{79}$$

which validates (77). The convergence (75) follows from inductively applying (72) to the left-hand side and summand terms in (77). ■

Next, we study the time-derivatives of the barrier functions.

Lemma 5: For $i = 2,\dots,n$ and $t \in [t_{2k-1}, T)$, we have that

$$\lim_{t\to T^-} \frac{\partial h_i(\underline{\mathbf{z}}_i, t)}{\partial t} = \lim_{t\to T^-} \mathcal{P}\left(\mu_1(t,T)\right)\xi_{i,2k-1}(t) = 0. \tag{80}$$

Proof: For $i = 2$, note that

$$\begin{aligned}\frac{\partial h_2(\underline{\mathbf{z}}_2, t)}{\partial t} &= \frac{\partial}{\partial t}\left(b^T\mathbf{z}_2 + c_2\mu_2(t,T)h_1(\mathbf{z}_1)\right) &(81)\\ &= \frac{2c_2}{T}\mu_3(t,T)h_1(\mathbf{z}_1) &(82)\end{aligned}$$

an application of (72) yields (80). Assume that (80) holds true for $i = j < n$; then

$$\begin{aligned}\frac{\partial h_{j+1}(\underline{\mathbf{z}}_{j+1}, t)}{\partial t} &= \frac{\partial}{\partial t}\left(\frac{d}{dt}h_j(\mathbf{z}_j, t) + c_j\mu_2(t,T)h_j(\mathbf{z}_j, t)\right) &(83)\\ &= \frac{d}{dt}\left(\frac{\partial h_j(\mathbf{z}_j, t)}{\partial t}\right) + \frac{2c_j}{T}\mu_3(t,T)h_j(\mathbf{z}_j, t) \\ &\quad + c_j\mu_2(t,T)\frac{\partial h_j(\mathbf{z}_j, t)}{\partial t} &(84)\end{aligned}$$

where commutativity follows from the structure of the backstepping transformation (20). An application of (72) and the induction hypothesis yields the result. ■

We can now study the sum within (25).

Lemma 6: For $i = 1,\dots,n-1$ and $t \in [t_{2k-1}, T)$, we have that

$$\begin{aligned}&\lim_{t\to T^-} \sum_{j=1}^{i} \frac{\partial h_i(\underline{\mathbf{z}}_i(t), t)}{\partial \mathbf{z}_j(t)}\mathbf{z}_{j+1(t)} \\ &= \lim_{t\to T^-} \mathcal{P}\left(\mu_1(t,T)\right)\xi_{i,2k-1}(t) = 0.\end{aligned} \tag{85}$$

Proof: We proceed by induction. For $i = 1$, the proof follows from (76). Assume (85) holds for $i = l-1$. Evaluating (20) at

$i = l$ yields

$$\sum_{j=1}^{l-1} \frac{\partial h_{l-1}}{\partial \mathbf{z}_j} \mathbf{z}_{j+1} = h_l(\underline{\mathbf{z}}_l, t) - \frac{\partial h_{l-1}}{\partial t} - c_{l-1}\mu_2 h_{l-1}. \quad (86)$$

Applying (69) and (72), and Lemma 5 to the right-hand side of the above leads to

$$\lim_{t\to T^-} \frac{d}{dt}\left(\sum_{j=1}^{l-1} \frac{\partial h_{l-1}}{\partial \mathbf{z}_j}\mathbf{z}_{j+1}\right) = \lim_{t\to T^-} \mathcal{P}\left(\mu_1(t,T)\right)\xi_{l-1,2k-1}(t) = 0. \quad (87)$$

Now, we consider the sum on the left-hand side of (85) for $i = l$

$$\sum_{j=1}^{l} \frac{\partial h_l}{\partial \mathbf{z}_j}\mathbf{z}_{j+1} = b^\top z_{l+1,\|} + \sum_{j=1}^{l-1} \frac{\partial h_l}{\partial \mathbf{z}_j}\mathbf{z}_{j+1} \quad (88)$$

and we use our backstepping transformation to rewrite

$$\begin{aligned}
\sum_{j=1}^{l-1} \frac{\partial h_l}{\partial \mathbf{z}_j}\mathbf{z}_{j+1} &= \sum_{j=1}^{l-1} \frac{\partial}{\partial \mathbf{z}_j}\left(\frac{d}{dt}h_{l-1} + c_{l-1}\mu_2 h_{l-1}\right)\mathbf{z}_{j+1} \\
&= \sum_{j=1}^{l-1}\left(\frac{d}{dt}\left(\frac{\partial h_{l-1}}{\partial \mathbf{z}_j}\right) + c_{l-1}\mu_2\frac{\partial h_{l-1}}{\partial \mathbf{z}_j}\right)\mathbf{z}_{j+1} \\
&\quad + \sum_{j=2}^{l-1} \frac{\partial h_{l-1}}{\partial \mathbf{z}_{j-1}}\mathbf{z}_{j+1} \\
&= \sum_{j=1}^{l-2}\left(\frac{d}{dt}\left(\frac{\partial h_{l-1}}{\partial \mathbf{z}_j}\right)\mathbf{z}_{j+1} + \frac{\partial h_{l-1}}{\partial \mathbf{z}_j}\mathbf{z}_{j+2}\right) \\
&\quad + \frac{d}{dt}\left(\frac{\partial h_{l-1}}{\partial \mathbf{z}_{l-1}}\right)\mathbf{z}_l + c_{l-1}\mu_2\sum_{j=1}^{l-1}\frac{\partial h_{l-1}}{\partial \mathbf{z}_j}\mathbf{z}_{j+1} \\
&= \frac{d}{dt}\left(\sum_{j=1}^{l-1}\frac{\partial h_{l-1}}{\partial \mathbf{z}_j}\mathbf{z}_{j+1}\right) \\
&\quad + c_{l-1}\mu_2\sum_{j=1}^{l-1}\frac{\partial h_{l-1}}{\partial \mathbf{z}_j}\mathbf{z}_{j+1}. \quad (89)
\end{aligned}$$

The ultimate term in (89) is convergent due to the induction hypothesis, and the penultimate term is convergent due to (87). Finally, the term corresponding to $j = l$ [i.e., the first term on the right-hand side of (88)] is itself convergent by (27) and by Lemma 4. ■

It is clear from (69), Lemma 5, and the proof of Lemma 6 [in particular, (89) evaluated at $l = n$, which gives a] that the overriding controller (30), which is generated by (25), is convergent for $t \in [t_{2k-1}, T)$, since

$$\lim_{t\to T^-} a(t) = 0. \quad (90)$$

Moreover, in the case that the overriding controller presides over (29) for $t \in [t_{2k-1}, T), k \in \mathbb{N}$, it converges to the following value at the terminal time:

$$\lim_{t\to T^-} v(t) = \left(I - \frac{bb^\top}{\|b\|^2}\right) v_{\text{nom}}(T). \quad (91)$$

The result (91) agrees with Lemma 4, since $(I - \frac{bb^\top}{\|b\|^2})v_{\text{nom}}(T) = v_{\text{nom},\perp}(T)$, since the parallel components of the feedback are driven to zero by this time. ■

Remark 2: We reiterate that while the treatment in this subsection was applied to the transformed system (18) in vector chain-of-integrator form, the designed PTSf controller achieves PTSf for the original vector strict-feedback system (1) via the input transformation (11) which retains the controller boundedness.

B. Solution Existence After Time T

When employing feedback gains that may grow unbounded, which is a fundamental feature of our PTSf design, the implications of such a design on closed-loop well posedness become significant. The prescribed-time attractivity that we achieve in (72) is a direct result of employing the time-varying gains in (25) that grow unbounded as $t \to T$. Nevertheless, by using (72) and Lemma 6 we have established that the product of these time-varying gains with the state feedback in (25) generates a continuous, T-uniformly bounded control law (29). In addition, we have shown in (75) that if v_{override} is the input signal to (18) in the interval $[\bar{t}, T)$, $0 \le \bar{t} < T$, the target system states $\mathbf{z}_{i,\|}(t)$, $i = 2, \ldots, n$, converge to zero as $t \to T$. Moreover, it follows from (72) that the first target system state $\mathbf{z}_1(t)$ converges to a unique constant vector $\mathbf{z}_1^*$ satisfying $h_1(\mathbf{z}_1^*) = 0$. Unique, because the system is driven by the solution to the QP problem (24) which is unique.

While the goal of PTSf is finite-time in nature, our algorithm may be used in applications where the time horizon extends past the terminal time. For scenarios when v_{nom} is the input signal presiding over (29) over the time interval $t \in [T - \epsilon, \infty)$ for $\epsilon > 0$, solution existence over this infinite time horizon reduces to v_{nom} being piecewise-continuous in t and Lipschitz in $\mathbf{z}$ [the diverging gains (25) are avoided]. For all other scenarios when v_{override} is the input signal to (18) over the time interval $\mathcal{T}_{T-\epsilon}^T := [T - \epsilon, T)$, solution existence and uniqueness is only guaranteed on $\mathcal{T}_0^T$.

We present arguments to extend this solution from $\mathcal{T}_0^T$ to an infinite time horizon. Smooth continuations of solutions can be performed using smooth partitions of unity via mollifiers [49]; particular to our time-varying treatment is that smooth solution extension is native to the solutions of the closed-loop system, since their convergence as $t \to T$ resembles those used for mollification of indicator functions.

Indeed, the function $\xi_{j,k}(t,T)$ in (75) is a smooth cutoff function with the convergence property (43). Extending this solution to the closed interval $[0, T]$ is then straightforward: using (43), we can invoke the Borel's theorem [[50], Thm. 1.2.6] to obtain existence of smooth functions (via power series) $\mathbf{z}_T(t)$ in a neighborhood of $t = T$ which agree with (75) and (72) (evaluated at $i = 1$, yielding the unique finite limits for $\mathbf{z}_1$). Since the target system (18) is a chain of integrators, its matrix exponential (which is generated by a nilpotent matrix) is readily computed. Using this matrix exponential, if $\mathbf{z}_i(T + \epsilon) = 0$ for $i = 2, \ldots, n$, then any solution $\bar{\mathbf{z}}_\infty(t)$ to (18) on the interval $[T + \epsilon, \infty)$ is only affected by the input $v(t)$, for any $\epsilon > 0$. Taking $\epsilon \to 0$, the solution $\bar{\mathbf{z}}_\infty(t)$ is compatible with the power series solution $\mathbf{z}_T(t)$ at time $t = T$, or $\bar{\mathbf{z}}_\infty(T) = \mathbf{z}_T(t)$. Hence,

the solution

$$\bar{\mathbf{z}}(t) = \begin{cases} \mathbf{z}(t), & t \in \mathcal{T}_0^T \\ \bar{\mathbf{z}}_\infty(t), & t \in \mathcal{T}_T^\infty \end{cases} \tag{92}$$

is the extension of $\mathbf{z}(t)$ to the infinite time horizon *with input* $v(t) = (I - \frac{bb^\top}{\|b\|^2})v_{\text{nom}}(t)$ according to (91).

However, as the notion of safety expires at $t = T$, we wish to cede the PTSf overriding authority to v_{nom} after this time. The target system (18) with $v(t)$ in (32) has a unique solution $\mathbf{z}_\infty(t)$ in $\mathcal{T}_{T+\epsilon}^\infty$ provided that v_{nom} is sufficiently regular. Moreover, the smooth cutoff function we employ in (34) gradually and smoothly applies the nominal input to the system such that $\lim_{\epsilon\to 0^+} v(T+\epsilon) = (I - \frac{bb^\top}{\|b\|^2})v_{\text{nom}}$ and $\lim_{\epsilon\to 0^-} v(T + \bar{T} + \epsilon) = v_{\text{nom}}$. As a result, we have that $\lim_{\epsilon\to 0^+} \mathbf{z}_\infty(T+\epsilon) = \bar{\mathbf{z}}(T)$, and that the nominal control input is implemented after an additional $\bar{T}$ units of time. Thus, it follows by uniqueness of both solutions that we can smoothly piece together a unique solution from $\bar{\mathbf{z}}(t)\big|_{[0,T]}$ and $\mathbf{z}_\infty(t)\big|_{(T,\infty]}$ over the infinite time horizon.

C. PTSf for Initially Unsafe Systems

We consider the dual problem of rescuing an initially unsafe system to safety in no later than an a-priori prescribed time T. In particular, suppose for the system (18) with output $y(t) = h(\mathbf{z}_1(t))$, the initial output satisfies $y(t_0) < -\varepsilon < 0$; we desire a controller that achieves

$$y(t_0 + T) \geq 0. \tag{93}$$

To proceed, we introduce the following assumption on the output map $h : \mathbb{R}^m \to \mathbb{R}$, which is a stronger version of Assumption 2

Assumption 3: The function $h : \mathbb{R}^m \to \mathbb{R}$ is n times differentiable and satisfies

$$\frac{\partial h}{\partial \mathbf{x}_1} \neq 0 \quad \forall \mathbf{x}_1 \in \mathbb{R}^m. \tag{94}$$

Corollary 7: If Assumption 3 holds, and if the system (18) is initially unsafe, that is, if $y(t_0) < -\varepsilon < 0$, then the control law (32), (19)–(34) ensures that $y(t_0 + T) \geq 0$ for the initial control gains selected as in (38) and (39). Moreover, the control law (32) is uniformly bounded provided that v_{nom} is continuous in the interval $[t_0, t_0 + T]$.

Proof: The proof follows by noticing that the barrier function definitions (20), choice of initial gains (38)–(39), and control law (32) lead to the same target system (36)–(37), but with initial condition $h_1(t_0) < 0, h_i(t_0) > 0$, for $i = 2, \ldots, n$. Using a similar argument, as in Theorem 1, we arrive at the same lower bound on $h_1(t)$ in (53) which leads to

$$y(t_0 + T) = h_1(t_0 + T) \geq 0. \tag{95}$$

The introduction of Assumption 3 ensures that the QP problem (24) remains feasible and that the controller boundedness argument in Theorem 1 applies. ■

V. Examples

We present three examples to demonstrate some fundamental properties and advantages of our PTSf design. To center attention on these properties of PTSf, we consider systems that are simple and theoretically well understood. For a more practical application of PTSf, see [51] which uses results from the conference version of this article for designing detailed experiments on a 7-degree of freedom (DOF) robot manipulator.

A. Double-Integrator Design Demonstration

Consider the double integrator

$$\dot{x}_1(t) = x_2(t) \tag{96}$$

$$\dot{x}_2(t) = u(t) \tag{97}$$

$$y(t) = -x_1(t), \quad t \geq t_0. \tag{98}$$

This system can be considered as an idealized model of the longitudinal dynamics of a vehicle, where the states x_1 and x_2 represent the position and velocity of the vehicle, respectively, and the input u represents the longitudinal acceleration/deceleration command. The safety objective is to enforce that the position x_1 remains negative for a prescribed time duration T during which the system is driven by a nominal control u_{nom} that can be overridden as needed to enforce safety. One possible application of this is the problem of ensuring that an ego vehicle does not violate a red traffic light that is on for a fixed duration T, irrespective of driver input. We begin the design by performing the time-varying backstepping transformation defined as follows:

$$\begin{aligned} h_1(x_1) &:= -x_1 \\ h_2(\underline{x}_2, t) &:= -x_2 + c_1\mu_2 h_1(x_1) \end{aligned} \tag{99}$$

where c_1 is a design parameter to be determined. The positivity of $h_1(x_1(t_0))$ follows from requiring that the system is initially safe, i.e., $x_1(t_0) < 0$. For $h_2(\underline{x}_2(t_0), t_0)$, we achieve positivity by choosing $c_1 > \max\{0, -\frac{x_2(t_0)}{x_1(t_0)}\}$, where we have used $\mu_2(t_0 - t_0, T) = 1$ in (99). Under the transformation (99) and the choice of control

$$\begin{aligned} u_{\text{override}} &= c_2\mu_2 h_2 + \frac{d}{dt}(c_1\mu_2 h_1) \\ &= -(c_1 + c_2)\mu_2 x_2 - c_1\left(c_2\mu_2 + \frac{2\mu_1}{T}\right)\mu_2 x_1 \end{aligned} \tag{100}$$

where $c_2 > 0$, the h-dynamics satisfy

$$\begin{aligned} \frac{d}{dt}h_1 &= -c_1\mu_2 h_1 + h_2 \\ \frac{d}{dt}h_2 &= -c_2\mu_2 h_2 \end{aligned} \tag{101}$$

which we have shown converges to the origin in T time units for positive constants c_1 and c_2 chosen to satisfy the aforementioned conditions. Thus, to enforce that the nominal control input u_{nom} does not make the state x_1 positive *before* time $t_0 + T$, we apply the safety filter

$$u = \begin{cases} u_{\text{safe}}, & \text{if } t_0 \leq t < t_0 + T \\ g(t, u_{\text{nom}}, 0, h_1(t_0 + T)), & \text{if } t \geq t_0 + T \end{cases} \tag{102}$$

where

$$u_{\text{safe}} = \min\{u_{\text{nom}}, u_{\text{override}}\} \tag{103}$$

and g is, as defined in (34). Strictly speaking, the safety filter $\min\{u_{\text{nom}}, u_{\text{override}}\}$ applied during times $t_0 \leq t < t_0 + T$ is the

solution of the QP problem

$$u_{\text{safe}} = \arg\min_{w\in\mathbb{R}} \ |w - u_{\text{nom}}|^2$$
$$\text{s.t. } w \le c_2\mu_2 h_2 + \frac{d}{dt}(c_1\mu_2 h_1) \tag{104}$$

where the inequality in (104) is equivalent to $\frac{d}{dt}h_2 + c_2\mu_2 h_2 \ge 0$ under input w.

1) PTSf Versus ESf: The Peaking Phenomenon: Suppose that the nominal control input u_{nom} is at risk of making the system unsafe, and we wish to design a *time-invariant* safety filter that overrides the nominal control and takes the system to the origin. This problem was studied in [21, Sec. 3.B] for input–output linearized systems via pole-placement (which inherently relies on the backstepping method—see [21, Rk. 5]), which achieves exponential convergence to the origin with arbitrary decay rate. We define the barrier functions

$$h_1(x_1) := -x_1$$
$$h_2(\underline{x}_2) := -x_2 + \rho h_1, \quad \rho > 0 \tag{105}$$

with the goal of keeping $h_1 \ge 0$ uniformly. Consider the following time-invariant safety filter designed as in [21]

$$u = \min\left\{u_{\text{nom}}, -\begin{pmatrix}2\rho^2 & 3\rho\end{pmatrix}x\right\}, \qquad \text{for } t_0 \le t < \infty \tag{106}$$

with $\rho \ge \max\{0, -\frac{x_2(t_0)}{x_1(t_0)}\}$. Suppose the safety filter overrides the nominal control input at $t = t_0 + \bar{t} < \infty$ and continues to enforce safety thereafter (i.e., $u(t) = -(2\rho^2 \ \ 3\rho)x(t)$ for all $t \ge t_0 + \bar{t}$, placing the closed-loop poles for the x-system at $\{-\rho, -2\rho\}$). Then the closed-loop system (96)–(98) is given by

$$x(t) = e^{-\rho(t-t_0-\bar{t})} \times \begin{pmatrix} 2 - e^{-\rho(t-t_0)} & \frac{1}{\rho} - \frac{e^{-\rho(t-t_0-\bar{t})}}{\rho} \\ 2\rho\left(e^{-\rho(t-t_0-\bar{t})} - 1\right) & 2e^{-\rho(t-t_0-\bar{t})} - 1 \end{pmatrix} x(t_0+\bar{t}). \tag{107}$$

If we wish to achieve large exponential decay when the system is unsafe, we can select $\rho \gg \max\{0, -\frac{x_2(t_0)}{x_1(t_0)}\}$ as large as desired. However, for small $t - t_0 - \bar{t}$, the righthand side of (107) can be very large depending on the size of ρ (in particular, x_2 grows with ρ). This illustrates the "peaking" phenomenon, which was studied for ODE control systems in [45], [46], and [47]. The celebrated work of Sussmann and Kokotovic [46] has exposed the possibility of disastrous outcomes in input–output feedback linearization, where rapid regulation of the output can have catastrophic consequences on the zero dynamics. Moreover, due to the structure of the feedback (106), even for systems with a full relative degree (systems without zero dynamics, as above), the control input becomes extremely large near time $t_0 + \bar{t}$.

In the context of safety, if (x_1, x_2) represent position and velocity, seeking time-invariant safety filters with large exponential decay ($\rho \gg \max\{0, -\frac{x_2(t_0)}{x_1(t_0)}\}$) results in a very large and rapid transient response in the velocity, which is undesirable as it causes a large "jerk" to the system.

For the time-varying safety filter (106), the control gains are chosen to initially start quite small and depending on the initial conditions [see (100)], and only grow very large simultaneously as the states get very small and as time approaches the prescribed terminal time. This eliminates the possibility of peaking.

2) Numerical Simulation: We now compare these results graphically to demonstrate the advantages of time-varying backstepping. We perform numerical simulations for the double-integrator system under the nominal controller

$$u_{\text{nom}} = -k_1\xi_1 - k_2\xi_2$$
$$\xi_1 = x_1 + a\sin(\omega t) + b$$
$$\xi_2 = x_2 + a\omega\cos(\omega t) \tag{108}$$

with $k_1 = k_2 = 4$, $a = 1$, $b = 0.8$, and $\omega = 2\pi/T$, where $T = 4$ is the prescribed time. The initial condition is chosen as $x(0) = (-4, 2)^\top$. For safety, we use the time-varying PTSf safety filter (102) and (100) with choice of gains $c_2 = c_1 = \max\{0, -\frac{x_2(0)}{x_1(0)}\} + 0.1 = 0.6$ and use ramp function (34) with $m = 2$ and $\bar{T} = 0.5$ for controller continuity at $t_0 + T$ [see Section III, (34) for details]. For comparison, we use the time-invariant ESf safety filter (106) with $\rho = 0.6$ and $\rho = 3.2$. The choice $\rho = 0.6$ was made to allow a gain equivalent to the initial gains $c_1\mu_2(0)$, $c_1\mu_2(0)$ of PTSf, and the choice $\rho = 3.2$ was tuned to make ESf less conservative and to react at around the same instant as PTSf.

For numerical stability near the origin, we clip the blow-up function μ_2 at a maximum value $\mu_{2,\max} = 1000$, which still allows the PTSf gains to grow to several orders of magnitudes larger than $\rho = 3.2$. This gain clipping is done for all numerical simulations in this article; and as a consequence, the systems under study are only allowed to reach a small neighborhood of the boundary of the safe set at the terminal time T. For a maximum gain $\mu_{2,\max} = 1000$ this neighborhood is sufficiently small and qualitatively insignificant. For all ODEs considered in this article, we use a simple first-order Euler method for numerical simulations; with a small sampling time of 10^{-5} due to the rapidly growing PTSf gains.

The system trajectories under PTSf and ESf are shown in Fig. 2, where we observe the ESf filter with $\rho = 0.6$ being overly restrictive, keeping the system further from its nominal trajectory. With ρ increased to 3.2, the ESf filter becomes less restrictive like PTSf but at the cost of a significantly higher jerk as evident in Fig. 3. Lastly, as evident in both figures, the PTSf filter eventually allows the system evolve freely after the prescribed time $T = 4$ has elapsed.

B. Vector-Valued Double Integrator With Nonlinear Constraint

To illustrate our design on a vector-valued chain of integrators, we consider the following system:

$$\dot{\mathbf{z}}_1 = \mathbf{z}_2$$
$$\dot{\mathbf{z}}_2 = \mathbf{v} \tag{109}$$

where $\mathbf{z}_1 = (z_{1,1}, z_{1,2})^\top$, $\mathbf{z}_2 = (z_{2,1}, z_{2,2})^\top$ are vector-valued states in $\mathbb{R}^2$, and $\mathbf{v} = (v_1, v_2)^\top$ is the vector-valued input. A nominal controller is designed to stabilize the states $(\mathbf{z}_1, \mathbf{z}_2)$ to the origin, while the safety condition is to keep the state $\mathbf{z}_1$ outside of a circular unsafe set, that is,

$$h(\mathbf{z}_1) = (z_{1,1} - c_1)^2 + (z_{1,2} - c_2)^2 - r^2 \tag{110}$$

where $(c_1, c_2) \in \mathbb{R}^2$ and $r \in \mathbb{R}$ are the center and radius of the unsafe-set, respectively. We apply the PTSf safety filter (32), (34), and (29) with initial gains $c_2 = c_1 = 1$ and terminal time

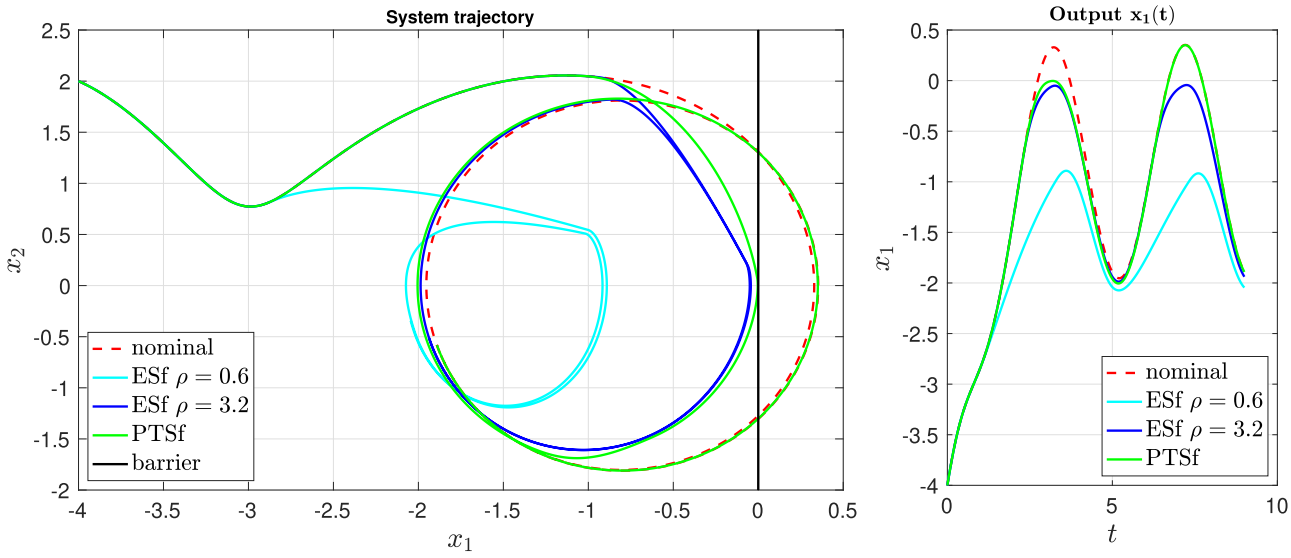

Fig. 2. System trajectories (left) and outputs (right) for double integrator under nominal controller (108) with initial condition $(x_1(0), x_2(0)) = (-4, 2)$ and prescribed terminal time $T = 4$ for safety. The PTSf safety filter uses (102) and (100) with $c_2 = c_1 = 0.6$ while the ESf safety filter uses (106) with $\rho = 0.6$ and $\rho = 3.2$ – the latter value tuned to make ESf react at the same instant as PTSf.

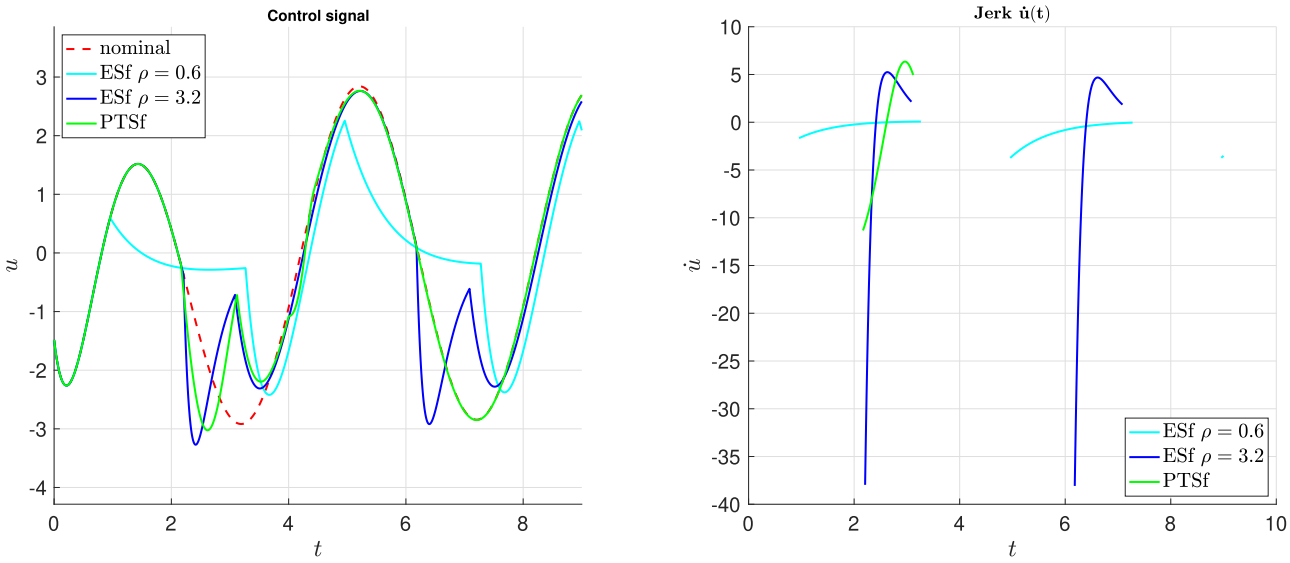

Fig. 3. Left: Control signal. Right: Jerk during intervals when nominal command is overridden. When ESf is tuned ($\rho = 3.2$ case) to be less restrictive like PTSf, the magnitude of the jerk increases significantly.

$T = 3$ with $\bar{T} = 0.5$, and compare with ESf filters designed similarly, as in Section V-A1, with $\rho = 1$ (matching the initial PTSf gains) and $\rho = 3$. The latter choice $\rho = 3$ was tuned so that under ESf, the system reaches the boundary of the unsafe set at about the same time as under the PTSf filter. In both cases (i.e., ESf with $\rho = 1$ and $\rho = 3$), the safety filter is turned OFFat the terminal time $T = 3$ and control authority returned to the nominal stabilizing controller using the cutoff function (34). The resulting system trajectories under the nominal controller, ESf safety filters, and PTSf safety filter are shown in Fig. 4, and in Fig. 5, we show the control effort exerted up until the terminal time $T = 3$ when all safety filters cede control authority to the nominal controller.

When the ESf filter ($\rho = 1$ case) is tuned to be as restrictive (in terms of control effort override) as PTSf at the initial time, the system deviates further from its nominal behavior due to the persistently low gain of the ESf filter which greatly limits the rate of approach to the boundary of the unsafe set over the time duration T. However, because PTSf uses gains that start small and grow large, it *initially* behaves like the slower (low-gain) ESf filter—permitting only a slow exponential approach rate to the barrier—but as time approaches the terminal time $T = 3$, behaves like a fast (high-gain) ESf filter and allows a fast exponential approach to the boundary of the safe set. By design, the system is guaranteed to be *able to* reach the boundary by time T under PTSf without the designer

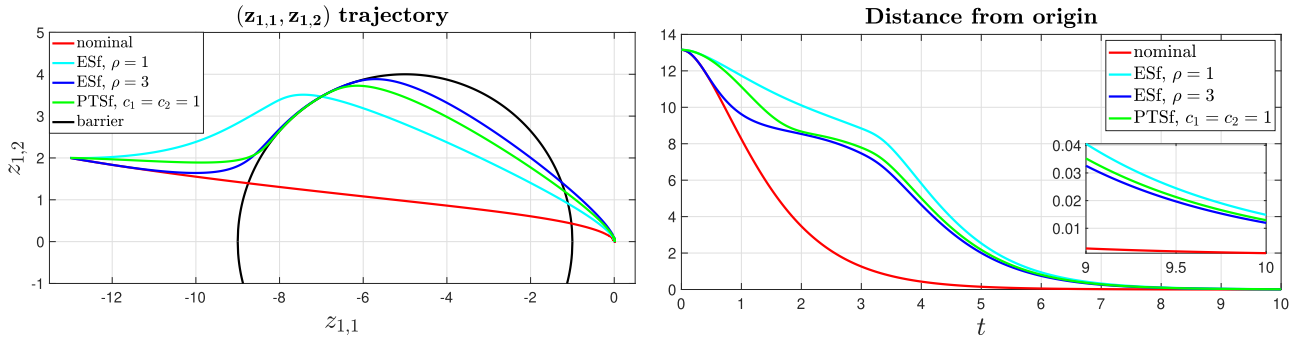

Fig. 4. System trajectories (left) and distance from origin (right) for the vector-valued double integrator (109) with initial condition $(z_{1,1}(0), z_{1,2}(0)) = (-13, 2)$, $(z_{2,1}(0), z_{2,2}(0)) = (0, 0)$ under a nominal stabilizing controller (red), a PTSf filter with terminal time $T = 3$ (green), and a ESf filers (cyan, blue).

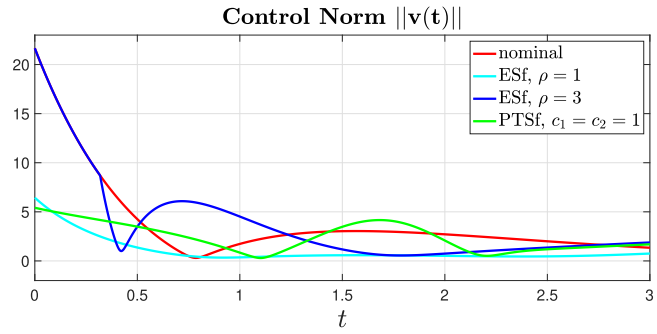

Fig. 5. Control signal for the vector-valued double integrator (109) with the PTSf safety filter with terminal time $T = 3$ applied.

needing to tune gains specifically for this purpose as is the case with ESf.

C. Preservation of Nominal Prescribed-Time Stabilization Performance

One advantage of PTSf safety filters over infinite-time ESf filters is the ability to enforce safety without destroying finite-time performance of the underlying nominal system. In particular, for systems where the nominal control objective is to be achieved in finite time as is the case in PTS, the ephemeral nature of PTSf makes it possible to enforce safety, and retain the finite properties of the nominal controller. To illustrate this advantage, we consider the following example. Consider the second order, scalar, strict-feedback system

$$\begin{aligned} \dot{x}_1(t) &= x_1^2(t) + x_2(t) \\ \dot{x}_2(t) &= u(t) \\ y(t) &= -x_1(t), \quad t \geq t_0. \end{aligned} \tag{111}$$

The safety-objective is to keep the system output $y(t)$ positive for all times $t \in [0, T)$, and the nominal control objective is to stabilize the system to the origin in prescribed time T_{nom}. We begin by transforming the system into double integrator form using state transformation $z_1(t) = x_1(t)$ and $z_2(t) = x_1^2(t) + x_2(t)$ leading to

$$\begin{aligned} \dot{z}_1(t) &= z_2(t) \\ \dot{z}_2(t) &= v(t) = u(t) + 2x_1(x_1^2 + x_2) \\ y(t) &= -z_1(t), \quad t \geq t_0. \end{aligned} \tag{112}$$

For the nominal control, we use a PTS controller, as in [52], for the transformed system. Specifically, we use

$$\begin{aligned} v_{\text{nom}}(t) &= -K\mu_2(t)z(t) \\ K &= \begin{bmatrix} \omega^2 & 2\zeta\omega \end{bmatrix} \end{aligned} \tag{113}$$

with $\omega = 4$ and $\zeta = 0.1$. Starting from initial state $(x_1(0), x_2(0)) = (-1, -1)$ which corresponds to $(z_1(0), z_2(0)) = (-1, 0)$, we apply ESf safety filters with $\rho = 1.2$ and $\rho = 10$, and the PTSf safety filter with initial gains $c_1 = c_2 = 1$ to the z-system and transform the resulting safe input to the x-system using

$$u(t) = v(t) - 2x_1(x_1^2 + x_2). \tag{114}$$

The slower ESf filter ($\rho = 1.2$) is tuned to be initially as restrictive as the PTSf filter, overriding the nominal input by roughly the same amount, while the faster ESf filter is chosen so that the output arrives sufficiently close to the boundary of the safe-region, thereby retaining the PTS property as much as possible. The resulting plots are shown in Fig. 6. While the PTSf safety filter initially limits the rate of approach to the $y(t) = 0$ boundary to enforce safety, it still preserves the PTS property of the nominal PTS controller. For the faster ESf safety filter with $\rho = 10$, the system gets sufficiently close to the boundary of the safe set at the terminal time; however, choosing the appropriate ESf gain ρ requires more effort from the designer, unlike in PTSf where the designer only chooses the terminal time to match the terminal time of the nominal PTS controller, and gains c_1 and c_2 according to the explicit prescription in (38).

Next, we explore the case where the terminal time for safety T is less than nominal prescribed stabilization time T_{nom}. This translates to a scenario where safety is desired for a time interval shorter than the prescribed stabilization time. Keeping the same initial conditions and initial control gains c_1 and c_2, we rerun the simulation with PTSf safety-filters with terminal times $T = 0.8,\ 0.6$, and 0.4 time units, respectively. The resulting system outputs and control signals are shown in Fig. 7, where we see the finite-time stabilization property of

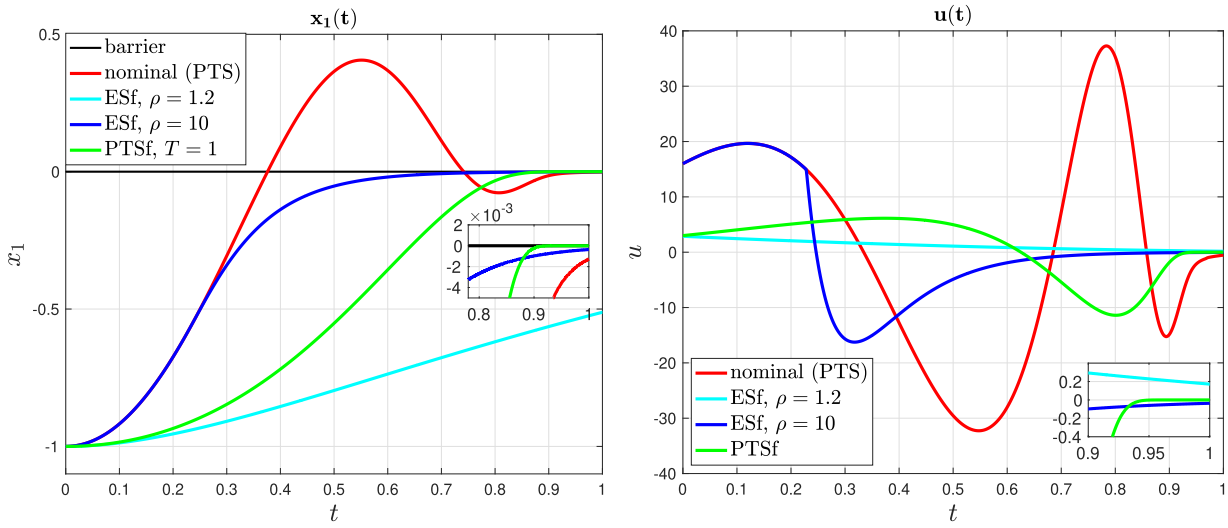

Fig. 6. Output (left) and input (right) for strict-feedback system (111) with initial condition $(x_1(0), x_2(0)) = (-1, -1)$ under nominal PTS controller (113) with terminal time $T_{\text{nom}} = 1$ (red), a PTSf filter with terminal time $T = 1$ (green), an ESf filter with $\rho = 1.2$ (cyan), and an ESf filter with $\rho = 10$ (blue).

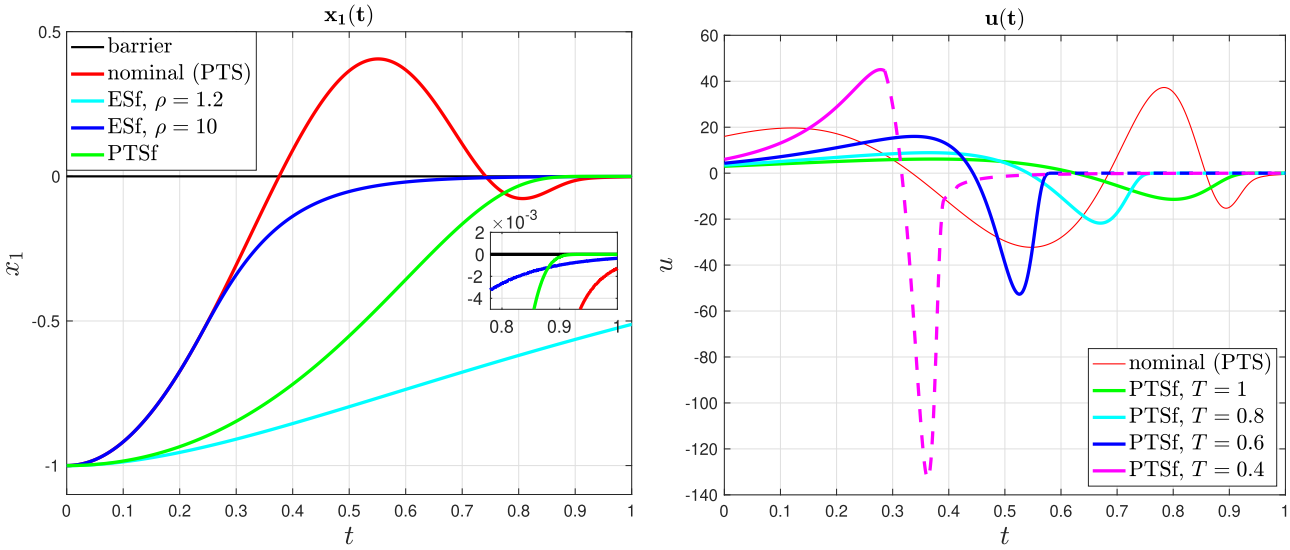

Fig. 7. Comparison of PTSf safety filters with terminal times $T \leq T_{\text{nom}} = 1$ of the nominal PTS controller. Dashed lines corresponds to periods when the nominal controller is not overridden; either because it is safe or because the safety interval T has elapsed.

the nominal controller being retained after the PTSf filters cede control.

VI. Conclusion

In this article, we present a safety filter design for strict-feedback systems that enforces state constraints for an a priori prescribed time. Our design uses a time-varying backstepping transformation with gains that grow as time approaches the terminal time. Despite the use of gains that grow toward infinity, we show that our safegaurding controller remains uniformly bounded provided that the nominal controller is uniformly bounded.

Absent from our treatment is the practical consideration of actuator constraints, which has been studied in, e.g., [53] and [54], where iterative methods *may* lead to the construction of viable safe sets if these methods converge; the nonexistence of viable safe sets given arbitrary actuator limitations is expected, and has been extensively studied for stabilization problems, e.g., [55] and [56].

Compelling future research directions include: studying predictor-based safety filter designs to compensate for input delays which are omnipresent in applications, developing output-feedback safety filters within the ISSf framework [5] and characterizing the relationship between estimation error and safety violations, characterizing and compensating for the effect of persistent disturbances appearing on the right-hand side of the dynamics, and developing a discretization algorithm that preserves the properties of our PTSf filter. Lastly, QP-based safety filters are only pointwise optimal and do not minimize a meaningful

cost function over the duration of safety enforcement. However, recent results on the design of inverse optimal (infinite-time) safety filters [57], inverse optimal prescribed-time stabilizing controllers [31], and CBF synthesis for approximate optimal control problems [58] have made promising the prospect of studying the design of inverse-optimal PTSf filters.

REFERENCES

[1] L. Wang, A. D. Ames, and M. Egerstedt, "Safety barrier certificates for collisions-free multirobot systems," *IEEE Trans. Robot.*, vol. 33, no. 3, pp. 661–674, Jun. 2017.

[2] M. Santillo and M. Jankovic, "Collision free navigation with interacting, non-communicating obstacles," in *Proc. Amer. Control Conf.*, 2021, pp. 1637–1643.

[3] P. Glotfelter, J. Cortés, and M. Egerstedt, "Nonsmooth barrier functions with applications to multi-robot systems," *IEEE Control Syst. Lett.*, vol. 1, no. 2, pp. 310–315, Oct. 2017.

[4] M. Jankovic, "Robust control barrier functions for constrained stabilization of nonlinear systems," *Automatica*, vol. 96, pp. 359–367, 2018.

[5] S. Kolathaya and A. D. Ames, "Input-to-state safety with control barrier functions," *IEEE Control Syst. Lett.*, vol. 3, no. 1, pp. 108–113, Jan. 2019.

[6] X. Xu, P. Tabuada, J. W. Grizzle, and A. D. Ames, "Robustness of control barrier functions for safety critical control," *IFAC-PapersOnLine*, vol. 48, no. 27, pp. 54–61, 2015.

[7] Y. Rahman, M. Jankovic, and M. Santillo, "Driver intent prediction with barrier functions," in *Proc. Amer. Control Conf.*, 2021, pp. 224–230.

[8] A. D. Ames, J. W. Grizzle, and P. Tabuada, "Control barrier function based quadratic programs with application to adaptive cruise control," in *Proc. IEEE Conf. Decis. Control*, 2014, pp. 6271–6278.

[9] X. Xu, J. W. Grizzle, P. Tabuada, and A. D. Ames, "Correctness guarantees for the composition of lane keeping and adaptive cruise control," *IEEE Trans. Automat. Sci. Eng.*, vol. 15, no. 3, pp. 1216–1229, Jul. 2018.

[10] T. G. Molnár, A. W. Singletary, G. Orosz, and A. D. Ames, "Safety-critical control of compartmental epidemiological models with measurement delays," *IEEE Control Syst. Lett.*, vol. 5, no. 5, pp. 1537–1542, Nov. 2021.

[11] I. Abel, M. Janković, and M. Krstić, "Constrained control of input delayed systems with partially compensated input delays," in *Proc. ASME Dyn. Syst. Controls Conf.*, 2020, pp. V001T04A006–7:8.

[12] M. Janković, "Control barrier functions for constrained control of linear systems with input delay," in *Proc. Amer. Control Conf.*, 2018, pp. 3316–3321.

[13] S. Prajna and A. Jadbabaie, "Methods for safety verification of time-delay systems," in *Proc. IEEE 44th Conf. Decis. Control*, 2005, pp. 4348–4353.

[14] A. Clark, "Control barrier functions for stochastic systems," *Automatica*, vol. 130, 2021, Art. no. 109688.

[15] S. Prajna, A. Jadbabaie, and G. J. Pappas, "A framework for worst-case and stochastic safety verification using barrier certificates," *IEEE Trans. Autom. Control*, vol. 52, no. 8, pp. 1415–1428, Aug. 2007.

[16] C. Santoyo, M. Dutreix, and S. Coogan, "A barrier function approach to finite-time stochastic system verification and control," *Automatica*, vol. 125, 2021, Art. no. 109439.

[17] P. Wieland and F. Allgöwer, "Constructive safety using control barrier functions," *IFAC Proc. Volumes*, vol. 40, no. 12, pp. 462–467, 2007.

[18] A. D. Ames, X. Xu, J. W. Grizzle, and P. Tabuada, "Control barrier function based quadratic programs for safety critical systems," *IEEE Trans. Autom. Control*, vol. 62, pp. 3861–3876, 2017.

[19] S.-C. Hsu, X. Xu, and A. D. Ames, "Control barrier function based quadratic programs with application to bipedal robotic walking," in *Proc. Amer. Control Conf.*, 2015, pp. 4542–4548.

[20] G. Wu and K. Sreenath, "Safety-critical and constrained geometric control synthesis using control Lyapunov and control barrier functions for systems evolving on manifolds," in *Proc. Amer. Control Conf.*, 2015, pp. 2038–2044.

[21] Q. Nguyen and K. Sreenath, "Exponential control barrier functions for enforcing high relative-degree safety-critical constraints," in *Proc. Amer. Control Conf.*, 2016, pp. 322–328.

[22] X. Xu, "Constrained control of input-output linearizable systems using control sharing barrier functions," *Automatica*, vol. 87, pp. 195–201, 2018.

[23] W. Xiao and C. Belta, "High-order control barrier functions," *IEEE Trans. Autom. Control*, vol. 67, no. 7, pp. 3655–3662, Jul. 2022.

[24] J. Breeden and D. Panagou, "High relative degree control barrier functions under input constraints," in *Proc. IEEE 60th Conf. Decis. Control*, 2021, pp. 6119–6124.

[25] M. Krstic and M. Bement, "Nonovershooting control of strict-feedback nonlinear systems," *IEEE Trans. Autom. Control*, vol. 51, no. 12, pp. 1938–1943, Dec. 2006.

[26] S. F. Phillips and D. E. Seborg, "Conditions that guarantee no overshoot for linear systems," *Int. J. Control*, vol. 47, no. 4, pp. 1043–1059, 1988.

[27] M. Bement and S. Jayasuriya, "Construction of a set of nonovershooting tracking controllers," *J. Dyn. Syst. Meas. Control*, vol. 126, no. 3, pp. 558–567, 2004.

[28] R. Schmid and L. Ntogramatzidis, "A unified method for the design of nonovershooting linear multivariable state-feedback tracking controllers," *Automatica*, vol. 46, no. 2, pp. 312–321, 2010.

[29] W. Li and M. Krstic, "Mean-nonovershooting control of stochastic nonlinear systems," *IEEE Trans. Autom. Control*, vol. 66, no. 12, pp. 5756–5771, Dec. 2021.

[30] Y. Song, Y. Wang, J. Holloway, and M. Krstic, "Time-varying feedback for regulation of normal-form nonlinear systems in prescribed finite time," *Automatica*, vol. 83, pp. 243–251, 2017.

[31] W. Li and M. Krstic, "Stochastic nonlinear prescribed-time stabilization and inverse optimality," *IEEE Trans. Autom. Control*, vol. 67, no. 3, pp. 1179–1193, Mar. 2022.

[32] N. Espitia, A. Polyakov, D. Efimov, and W. Perruquetti, "Boundary time-varying feedbacks for fixed-time stabilization of constant-parameter reaction-diffusion systems," *Automatica*, vol. 103, pp. 398–407, 2019.

[33] D. Steeves, M. Krstic, and R. Vazquez, "Prescribed-time h^1-stabilization of reaction-diffusion equations by means of output feedback," in *Proc. 18th Eur. Control Conf.*, 2019, pp. 1932–1937.

[34] D. Steeves, M. Krstic, and R. Vazquez, "Prescribed–time estimation and output regulation of the linearized Schrödinger equation by backstepping," *Eur. J. Control*, vol. 55, pp. 3–13, 2020.

[35] N. Espitia, D. Steeves, W. Perruquetti, and M. Krstic, "Sensor delay-compensated prescribed-time observer for LTI systems," *Automatica*, vol. 135, 2022, Art. no. 110005.

[36] D. Steeves and M. Krstic, "Prescribed-time stabilization of odes with diffusive actuator dynamics," *IFAC-PapersOnLine*, vol. 54, no. 9, pp. 434–439, 2021.

[37] D. Steeves, N. Espitia, M. Krstic, and W. Perruquetti, "Input delay compensation in prescribed-time of boundary-actuated reaction-diffusion PDEs," in *Proc. Amer. Control Conf.*, 2021, pp. 274–279.

[38] V. T. Haimo, "Finite time controllers," *SIAM J. Control Optim.*, vol. 24, no. 4, pp. 760–770, 1986.

[39] A. Polyakov, D. Efimov, and W. Perruquetti, "Finite-time and fixed-time stabilization: Implicit Lyapunov function approach," *Automatica*, vol. 51, pp. 332–340, 2015.

[40] I. Salehi, G. Rotithor, and A. Dani, "Safe adaptive trajectory tracking control of robot for human-robot interaction using barrier function transformation," in *Collaborative and Humanoid Robots*. London, U.K.: IntechOpen, 2021, Art. no. 129.

[41] A. Polyakov and M. Krstic, "Finite- and fixed-time nonovershooting stabilizers and safety filters by homogeneous feedback," *IEEE Trans. Autom. Control*, vol. 68, no. 11, pp. 6434–6449, Nov. 2023, doi: 10.1109/TAC.2023.3237482.

[42] M. Ohnishi, G. Notomista, M. Sugiyama, and M. Egerstedt, "Constraint learning for control tasks with limited duration barrier functions," *Automatica*, vol. 127, 2021, Art. no. 109504.

[43] K. Garg, R. K. Cosner, U. Rosolia, A. D. Ames, and D. Panagou, "Multi-rate control design under input constraints via fixed-time barrier functions," *IEEE Control Syst. Lett.*, vol. 6, pp. 608–613, 2022.

[44] L. Kong, W. He, Z. Liu, X. Yu, and C. Silvestre, "Adaptive tracking control with global performance for output-constrained MIMO nonlinear systems," *IEEE Trans. Autom. Control*, vol. 68, no. 6, pp. 3760–3767, Jun. 2023.

[45] H. Kimura, "A new approach to the perfect regulation and the bounded peaking in linear multivariable control systems," *IEEE Trans. Autom. Control*, vol. 26, no. 1, pp. 253–270, Feb. 1981.

[46] H. Sussmann and P. Kokotovic, "The peaking phenomenon and the global stabilization of nonlinear systems," *IEEE Trans. Autom. Control*, vol. 36, no. 4, pp. 424–440, Apr. 1991.

[47] H. K. Khalil and F. Esfandiari, "Semiglobal stabilization of a class of nonlinear systems using output feedback," in *Proc. IEEE 31st Conf. Decis. Control*, 1992, pp. 3423–3428.

[48] I. Abel, D. Steeves, M. Krstić, and M. Jankovi'c, "Prescribed-time safety design for a chain of integrators," in *Proc. Amer. Control Conf.*, 2022, pp. 4915–4920.

[49] W. Rudin et al. *Principles of Mathematical Analysis*, vol. 3. New York, NY, USA: McGraw-Hill, 1976.
[50] L. Hörmander, *The Analysis of Linear Partial Differential Operators I: Distribution Theory and Fourier Analysis*. Berlin, Germany: Springer, 2015.
[51] A. Bertino, P. Naseradinmousavi, and M. Krstić, "Prescribed-time safety filter for a 7-DoF robot manipulator: Experiment and design," *IEEE Trans. Control Syst. Technol.*, vol. 31, no. 4, pp. 1762–1773, Jul. 2023.
[52] P. Krishnamurthy, F. Khorrami, and M. Krstić, "Robust adaptive prescribed-time stabilization via output feedback for uncertain nonlinear strict-feedback-like systems," *Eur. J. Control*, vol. 55, pp. 14–23, 2020.
[53] D. R. Agrawal and D. Panagou, "Safe control synthesis via input constrained control barrier functions," in *Proc. IEEE 60th Conf. Decis. Control*, 2021, pp. 6113–6118.
[54] J. Breeden and D. Panagou, "Compositions of multiple control barrier functions under input constraints," in *Proc. Amer. Control Conf.*, 2023, pp. 3688–3695.
[55] A. R. Teel, "Global stabilization and restricted tracking for multiple integrators with bounded controls," *Syst. Control Lett.*, vol. 18, no. 3, pp. 165–171, 1992.
[56] H. Sussmann, E. Sontag, and Y. Yang, "A general result on the stabilization of linear systems using bounded controls," in *Proc. IEEE 32nd Conf. Decis. Control*, 1993, pp. 1802–1807.
[57] M. Krstic, "Inverse optimal safety filters," *IEEE Trans. Autom. Control*, early access, May 22, 2023, doi: 10.1109/TAC.2023.3278788.
[58] M. H. Cohen and C. Belta, "Approximate optimal control for safety-critical systems with control barrier functions," in *Proc. IEEE 59th Conf. Decis. Control*, 2020, pp. 2062–2067.

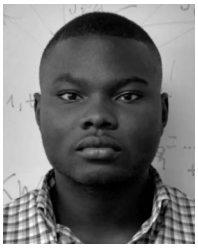

Imoleayo Abel received the B.S. degree in engineering and B.A. degree in computer science with High Honors in General Engineering and Computer Science from Swarthmore College, Swarthmore, PA, USA, in 2014, and the M.S. and Ph.D. degrees in mechanical engineering from the University of California San Diego, La Jolla, CA, USA, in 2018 and 2022, respectively.

His research interests include control theory, safety critical control, delay systems, and autonomous vehicle control.

Drew Steeves received the bachelor's and master's degrees in mathematics and engineering with Queen's University in Ontario, Kingston, ON, Canada, in 2015 and 2017, and the Ph.D. degree in dynamics and control with the University of California, San Diego, La Jolla, CA, USA, in 2022.

His research interests include high-performance control and estimation designs for time-enhanced convergence, safety-critical control, and under-actuated control systems.

Dr. Steeves was the recipient of the SIAM CST Best SICON Paper Prize in 2021 for his published Master's thesis.

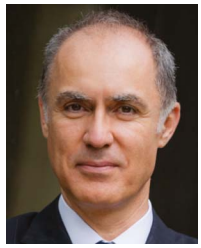

Miroslav Krstić (Fellow, IEEE) received the B.S. degree in electrical engineering from the University of Belgrade, in 1989, the M.S. and Ph.D. degrees in electrical engineering, University of California, Santa Barbara, in 1992 and 1994.

He is Distinguished Professor of Mechanical and Aerospace Engineeringwith the University of California San Diego (UCSD), La Rolla, CA, USA, where he holds the Alspach endowed chair, and is the founding Director of the Cymer Center for Control Systems and Dynamics. He also serves as Senior Associate Vice Chancellor for Research with UCSD. He has coauthored eighteen books in the areas of his research interests. He has edited two Springer book series. His research interests include adaptive, nonlinear, and stochastic control, extremum seeking, control of PDE systems including turbulent flows, and control of delay systems.

Dr. Krstic is the Fellow of International Federation of Automatic Control, American Society of Mechanical Engineers, Society for Industrial and Applied Mathematics, American Association for the Advancement of Science, Institution of Engineering and Technology (U.K.), and the Associate Fellow of American Institute of Aeronautics and Astronautics, and a Foreign Member of the Serbian Academy of Sciences and Arts and of the Academy of Engineering of Serbia. As a graduate student, he was the recipient of the UC Santa Barbara best dissertation award and student best paper awards at CDC and ACC. He was also the recipient of the Richard E. Bellman Control Heritage Award, Bode Lecture Prize, SIAM Reid Prize, ASME Oldenburger Medal, Nyquist Lecture Prize, Paynter Outstanding Investigator Award, Ragazzini Education Award, IFAC Nonlinear Control Systems Award, IFAC Ruth Curtain Distributed Parameter Systems Award, IFAC Adaptive and Learning Systems Award, Chestnut textbook prize, AV Balakrishnan Award for the Mathematics of Systems, Control Systems Society Distinguished Member Award, the PECASE, NSF Career, and ONR Young Investigator awards, the Schuck in 1996 and 2019 and Axelby paper prizes, and the first UCSD Research Award given to an engineer. He was also the recipient of the Springer Visiting Professorship at UC Berkeley, the Distinguished Visiting Fellowship of the Royal Academy of Engineering, the Invitation Fellowship of the Japan Society for the Promotion of Science, and four honorary professorships outside of the United States. He currently serves as the Editor-in-Chief for *Systems & Control Letters* and has been serving as the Senior Editor for *Automatica* and IEEE TRANSACTIONS ON AUTOMATIC CONTROL. He has served as the Vice President for Technical Activities of IEEE Control Systems Society and as Chair of the IEEE CSS Fellow Committee.

Mrdjan Janković (Fellow, IEEE) received his undergraduate degree in electrical engineering from Belgrade University, in 1987, and doctoral degree in systems science from Washington University, St. Louis, in 1992.

He held postdoctoral positions with Washington University and UC Santa Barbara, before joining Ford in 1995. From 1995 to 2022 he held progressively higher level technical leadership positions at Ford Research, working on development of control technologies for powertrain and driver assist applications. Dr. Jankovic coauthored one book, five book chapters, and more than 140 external technical papers. He is a co-inventor on 93 US patents, with 25 used in Ford products sold worldwide.

Dr. Jankovic received IFAC Nichols Medal, AACC Control Engineering Practice Award, IEEE Control Systems Technology Award, Fords prestigious Dr. Haren Gandhi Research and Innovation Award, and best paper awards from IEEE, SAE, and AVEC. Dr. Jankovic is a Fellow of the IEEE and a member of the National Academy of Engineering.